

MICROEARTHQUAKE SEISMICITY AND FAULT PLANE SOLUTIONS IN THE HINDU KUSH REGION  
AND THEIR TECTONIC IMPLICATIONS

J. L. Chatelain,<sup>1</sup> S. W. Roecker,<sup>2</sup> D. Hatzfeld,<sup>1</sup> and P. Molnar<sup>2</sup>

**Abstract.** The nature of the Hindu Kush intermediate seismic zone was studied in two microearthquake investigations in 1976 and 1977. By testing several sources of uncertainty the precision of about 600 earthquake locations was estimated to be about 5 km in epicenter and 10 km in depth. Projections of the earthquake locations from several perspectives reveal several regions of aseismicity as well as a highly contorted nature of the active regions. Very little seismicity was recorded in the crust from 0- to 70-km depth. The part of the zone southwest of about 37°N, 71.5°E and shallower than about 160 km is broad and seems to dip north at progressively steeper angles from west to east. Fault plane solutions for this region do not reveal a simple consistent pattern. This region is separated from another active region to the northeast by a curved gap that is nearly 50 km wide. Northeast of this gap the zone dips to the southeast. In the western portion there is an aseismic region around 160-km depth that separates the contorted shallower zone from a narrow (15-20 km wide), consistently steep, deeper zone. As in island arcs, the fault plane solutions for the deeper events show T axes generally lying within the plane of seismicity and P axes perpendicular to the plane. In contrast to island arcs the T axes in general are not parallel to the dip direction, and there seems to be greater variation in the orientation of these axes. The entire western zone plunges to the west at about 20°, and most of the T axes plunge steeply to the west. In detail, the earthquakes tend to occur in clusters that leave aseismic gaps between the clusters. There is a distinct gap of about 15-km width near 70.7°E. This gap seems to separate events with fault plane solutions that in the west have westward plunging T axes and in the east have eastward or vertically plunging T axes. Although many of these features were not detected in previous studies of this region, the data from those studies are consistent with the dips, changes in dip, gaps, and breadth of the seismic zone. Both the variations in dip and breadth of the active zones and, for one gap, the difference in fault plane solutions of earthquakes on either side of it, make the role of the gaps as boundaries clear and suggest their long-term existence. We infer that the configuration of the Hindu Kush seismic zone could possibly be the result of the subduction of oceanic litho-

sphere from two separate, small basins in opposite directions. The age of the subducted lithosphere is probably greater than 70 m.y., and subduction probably has occurred over a relatively short duration. The rate of subduction probably has been between 20 mm/yr and 48 mm/yr. Correlations of seismic trends with surficial features suggest that in the south the Hindu Kush suture zone lies along or somewhere between the Panjer and Kunar faults and that in the north the Pamir suture zone lies near the Darvaz-Karakul fault. Finally, it seems that the protrusion of India into Eurasia has been a major factor in developing the present configuration of the zone.

Introduction

The upper mantle beneath the mountainous Hindu Kush region of northeastern Afghanistan is the site of a tectonically complex area. Although it is not clearly associated with any island arc system, this region is perhaps the most active zone of intermediate depth (70-300 km) earthquakes in the world. The region is therefore interesting, since it provides a setting for examining deep-seated tectonic processes in a collision zone as well as allowing a study of intermediate depth seismicity as a phenomenon in itself.

Because of its proximity to the Eurasian-Indian plate boundary the Hindu-Kush seismic zone is believed to be grossly related to the convergence of the Indian and Eurasian subcontinents. The scenarios offered by various authors for the existence of the zone, however, cover a wide spectrum. Many authors [Billington et al., 1977; Isacks and Molnar, 1971; Khalaturin et al., 1977; Nowroozi, 1971, 1972; Santo, 1969] have suggested that the zone is evidence of subducted oceanic lithosphere, possibly remnants either of the Tethys Sea or of a marginal interarc basin. Explanations of this type are complicated by the unusual configuration of the zone, which seems to be much more contorted than is typical of island arcs, and other interpretations have been given. Santo [1969], for example, on the basis of what he interpreted to be a V-shaped zone of seismicity, suggested that two lithospheric layers had been underthrust from different directions in the same place. Alternatively, Vinnik et al. [1977] and Vinnik and Lukk [1973, 1974] interpret the activity as the result of a downward extension of a Paleozoic shieldlike structure. In their scenario this structure defines a 300-km-thick tectosphere that is being stressed by compressive forces somehow associated with the Himalayan fold belt. The wide range of explanations is indicative of a lack of conclusive evidence, such as large numbers of precisely determined earthquake locations or compatible relations to surficial geology.

<sup>1</sup>Laboratoire de Geophysique Interne, Institute de Recherches Interdisciplinaires de Geologie et de Mechanique, B.P. 53, 38041 Grenoble, France.

<sup>2</sup>Department of Earth and Planetary Sciences, Massachusetts Institute of Technology, Cambridge, Massachusetts 02139.

To help resolve the origin of the intermediate seismic zone, we carried out investigations of microearthquakes in the Hindu Kush region in both 1976 and 1977. Our immediate objectives were to define accurately the configuration of the seismic zone and to determine more fault plane solutions of earthquakes of the region over a larger portion than has been possible using data from the World-Wide Standardized Seismic Network (WWSSN) alone. Despite the short duration of these studies - 2 weeks in 1976 and 1 month in 1977, the high activity of the area (40 locatable events per day) made these objectives feasible. In order to infer the long-term nature of some of the features in the seismicity we compare the results of these investigations with those from previous studies made of the Hindu Kush region. These include the results of a 2-year microearthquake study by Soviet scientists in 1966-1967 [Roecker et al., 1980] as well as the teleseismic studies of Billington et al. [1977] and Santo [1969].

Data

#### Recording Procedure

From June 11 to July 13, 1977, we operated 11 Sprengnether MEQ-800 smoked paper recording systems circling the Hindu Kush in north-eastern Afghanistan (Figure 1). In addition, we obtained copies of short-period records from the Seismic Research Observatory (KBL) in Kabul. The stations were distributed to allow precise locations of intermediate depth (70-300 km) events. However, owing to various geographical and political limitations (e.g., bad roads and proximity to borders with neighboring countries) we were unable to put stations further east or north of the zone. Nevertheless, the wide range of takeoff angles along with adequate recording of the other azimuths seems to compensate for lack of coverage on the north and east.

The Sprengnether stations operated

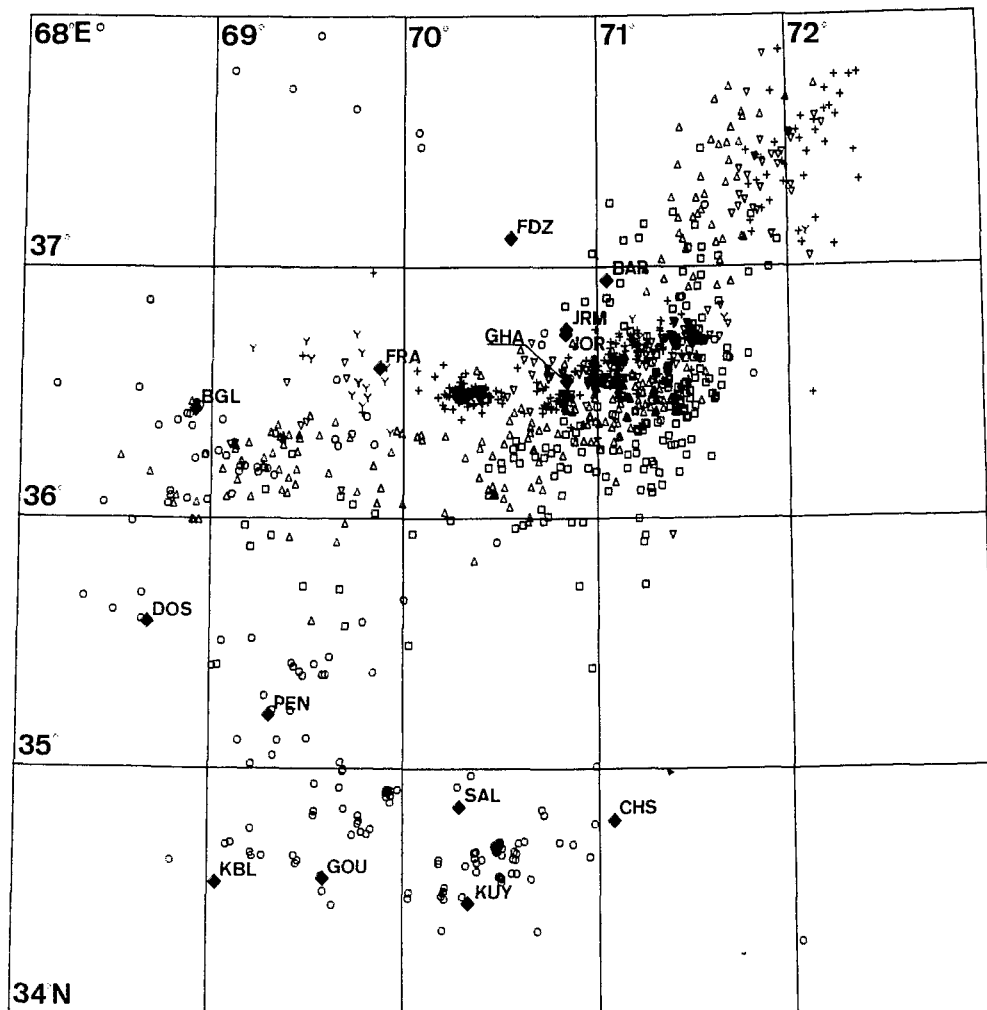


Fig. 1. Arrangement of seismographs and location of epicenters during the 1977 investigation. Station locations are indicated by solid diamonds. The epicenters are plotted with symbols corresponding to depth ( $z$ ) intervals as follows: open circles,  $0 \leq z \leq 50$  km; squares,  $50 \leq z \leq 100$  km; triangles,  $100 \leq z \leq 150$  km; inverted triangles,  $150 \leq z \leq 200$  km; pluses,  $200 \leq z \leq 250$  km; and y's,  $z \geq 250$  km.

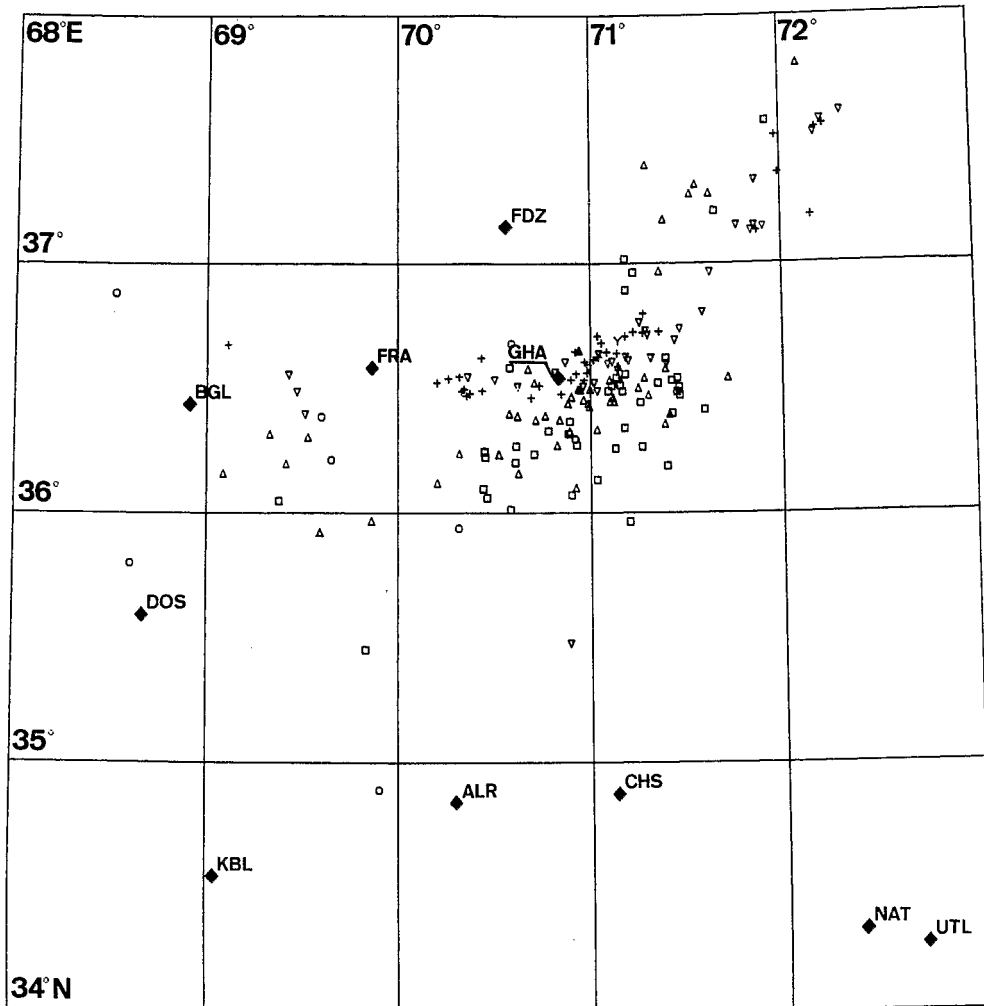


Fig 2. Arrangement of seismographs and location of epicenters during the 1976 investigation. Symbols for stations and epicenters are the same as in Figure 1.

continuously throughout the duration of the investigation. All of the stations were equipped with 1-Hz L4-C vertical seismometers. The filters on the instruments were set to allow a flat velocity response to frequencies between 0.3 and 30 Hz, and the amplifier gains were set at either 78 or 84 dB. The amplification of the signal from the ground motion to the trace on the record is about 500,000 at 84 dB and 250,000 at 78 dB. Traces were recorded by a fine stylus on kerosene smoked paper fixed to a rotating drum. The drum rotated at 60 mm/min at most stations and 120 mm/min at KUY. The records were changed every 2 days at all stations except KUY (which was maintained daily) and the clock drift was checked by recording a time signal transmitted by the ATA station in New Delhi. Station locations were determined using topographic maps with a scale of 1:250,000. The short-period records obtained from KBL were in ink and were recorded at 120 mm/min. Maintenance on these instruments was performed daily by members of Kabul University. The data accumulated during this investigation will be the primary topic in the discussion below.

A preliminary field study for the work in

1977 was made between August 18 and 31, 1976 [Chatelain et al., 1977]. During that time we operated seven stations in a configuration similar to that in 1977 (Figure 2). The field procedure was essentially the same as that in 1977. These data were supplemented by recordings from short- (and sometimes long) period instruments in Kabul and from the Lamont-Doherty array near Tarbella Dam [Armbruster et al., 1978].

#### Analysis of Data

In Appendix A<sup>1</sup> we give an extended discussion of the procedures used to analyze the seismograms, the reasoning behind our estimates of the uncertainties in the arrival times, a long discussion of the tests made to evaluate errors in locating the events, and the logic behind the criteria used to assign uncertainties

<sup>1</sup>Appendix is available with entire article on microfiche. Order from the American Geophysical Union, 2000 Florida Ave., N. W., Washington, DC 20009. Document J80-002; \$01.00. Payment must accompany order.

TABLE 1. Velocities of Layered Model Used to Locate Events

Depth to Top of Layer, km	Velocity of P Wave, km/s
0	6.0
45	8.0
85	8.2
110	8.4
150	8.6
200	8.8

to the location. Here we summarize the results described in Appendix A.

To analyze the 170 seismograms with nearly 45,000 arrivals, we digitized, on a tabletop digitizer, the phases of interest and relevant minute marks. A computer program then computed arrival times. We estimate the uncertainty of impulsive P arrivals to be about 0.1 s and emergent ones to be about 0.2 s, after clock corrections have been added. We used S phases whenever we could confidently pick the onset with an uncertainty of less than 1 s.

To evaluate the uncertainties in the locations, a series of tests were made, using both synthetic and real data. The first test was designed to examine whether or not the program HYP071 [Lee and Lahr, 1975], which assumes a flat layered structure, could locate events well in a region as large as the Hindu Kush (dimensions 300 km). Travel times to stations from hypothetical events at different locations were calculated for a spherical earth, and the events were relocated with HYP071. Epicenter had errors less than 0.5 km, and depths were wrong by about 1 km (Table A1). We conclude that the dimensions of the Hindu Kush region pose no obstacle to HYP071.

The second test explored the effects of random errors on the location. Travel times were calculated to stations for 58 events throughout the zone, and the events were relocated after random errors of 0.1 s for P and 0.6 s for S were added to the synthetic data. The mean mislocation is about 2 km but increases toward the edge of the array to 3 km (Table A2). When standard errors were increased to 0.2 and 1.0 s for P and S, the mislocation increased by about 1 km throughout the array (Table A3).

We then made tests with subsets of the array to determine the precision of the location and to gain insight into which data were redundant. We first selected 15 well-recorded events throughout the array and relocated them with subsets of the stations used initially (Table A4). Provided S waves were used, and provided 8 or more arrivals were used, locations were generally within 2-3 km of one another. Without an S wave the locations were much less reliable. Similar results were found by Buland [1976] and James et al. [1969]. The geometry of the network also is very important. To insure reliable depths, the distance of one station to the epicenter should be less than the depth. Moreover, when the azimuths to all

stations are within 60° of one another, more than eight arrivals are needed. As a second method we calculated uncertainties in location using the covariance matrix relating the data and location (see Appendix A and Figure A1). Results of this analysis agree with those described above and suggest that eight phases, including at least one S phase, are adequate to give a precision of 2-3 km in the locations in most of the region.

Because there are likely to be large lateral heterogeneities in the deep structure of the Hindu Kush while HYP071 requires a flat layered structure, we also calculated travel times from hypothetical events in a laterally heterogeneous structure and relocated them with HYP071. The heterogeneous structure was intended to imitate a slab of high-velocity material with maximum velocity contrast of 10%, surrounding the earthquake zone (Figure A2). This was imbedded in the uniform structure used by HYP071 (Table 1), a modification of that given by Lukk and Nersesov [1970]. The results show that relocations (Table A5) are in error by less than 5 km. When an incorrect choice of the ratio  $V_p/V_s$  was assumed (1.70 or 1.76 instead of 1.74), however, the relocated depths were systematically in error by about 10 km (too deep for  $V_p/V_s = 1.70$  and too shallow for 1.76). These errors are systematic, so in terms of the precision of the locations the effect of the lateral heterogeneity introduces an error of about 5 km.

All of the results discussed above apply to events in the center of the array. For the deeper events in the western portion, however, the uncertainties could be twice as large.

From these tests we considered as reliable only locations based on at least eight arrivals, with at least one S phase and with at least one station at a distance from the epicenter less

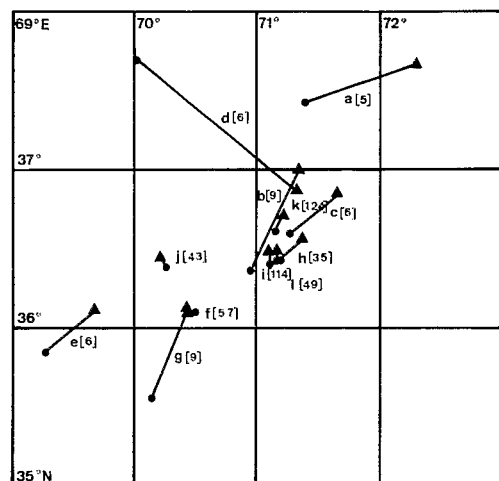


Fig. 3. A comparison of event epicenters located by both the USGS and the 1977 local array. Solid circles are epicenters reported by the USGS, and solid triangles are epicenters located by the local array. Letters near the epicenters specify the events in Table A7. Numbers in brackets refer to the number of stations used by the USGS in locating the events.

than the depth of focus. In addition, when the azimuths to all the stations were within only 60°, only those locations based on 10 or more such stations were considered reliable. Finally, acceptable locations included only those with root-mean-square residuals (Rms) greater than 0.1 s but less than 0.55 s. Among 1200 initial locations we used only 600. They are listed in Table A6.

We estimate the uncertainties in the epicenter to be about 5-10 km, increasing with a decreasing number of arrivals and decreasing depth. Similarly, depths are uncertain by

5-15 km. For comparison we plotted the locations of events in 1976 and 1977 that were also located by the United States Geological Survey (USGS) (Figure 3 and Table A7). The locations given by USGS for events recorded at more than 40 stations differ by about 10 km in depth and about 5 km in epicentral coordinates from those obtained by the local arrays. USGS locations with less than 40 stations disagree with ours considerably. Agreement in location suggests that both locations are good and that many stations are required to locate an event well teleseismically.

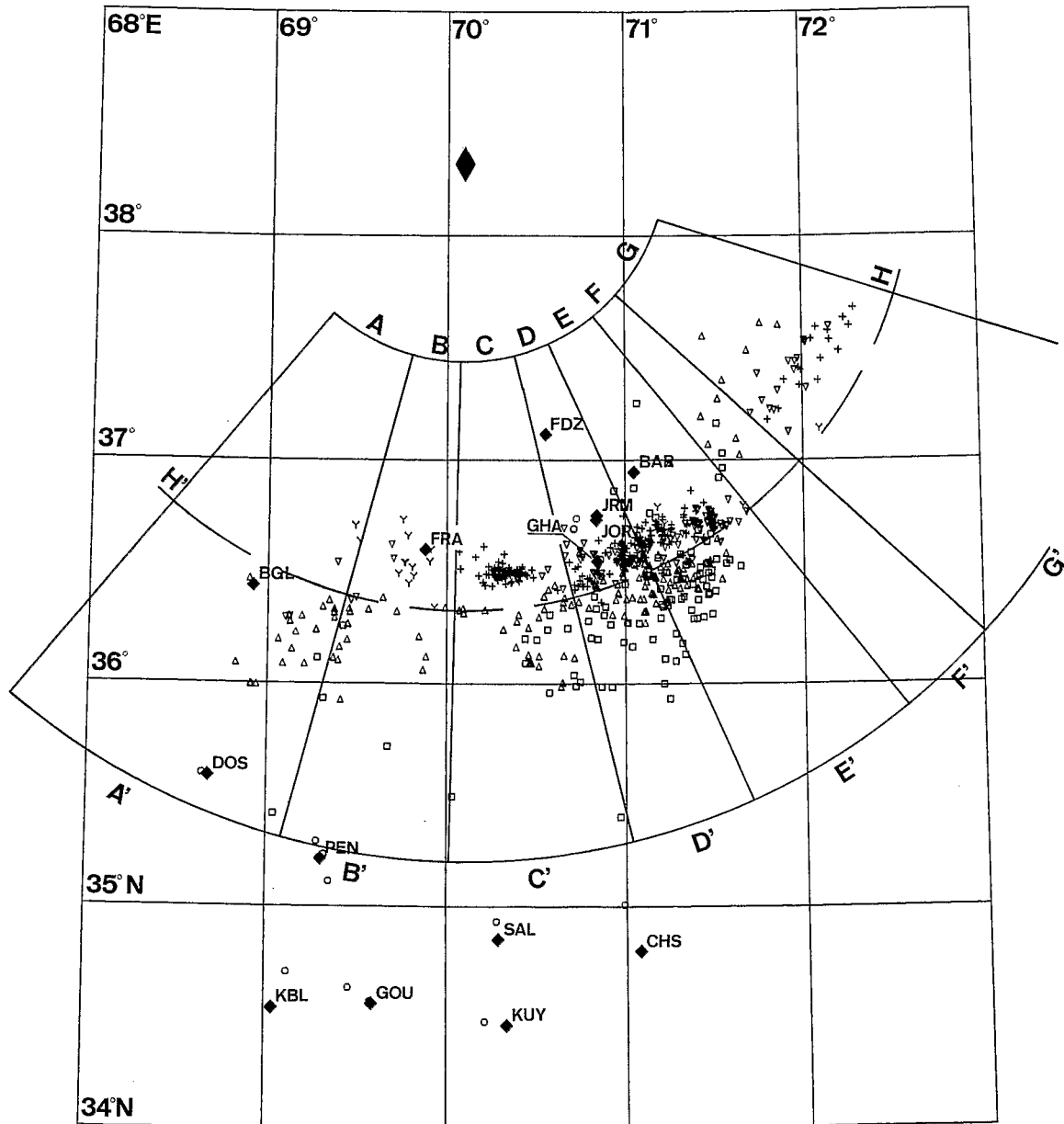


Fig. 4. Map view of the earthquake locations which passed all the quality criteria, along with the plotting scheme for cross sections. In plotting cross sections perpendicular to the trend of the zone, hypocenters are projected onto planes which bisect the sections. The lateral cross section is made by radially projecting hypocenters onto a vertical cylinder, the intersection of which with the map is denoted by the line H'H.

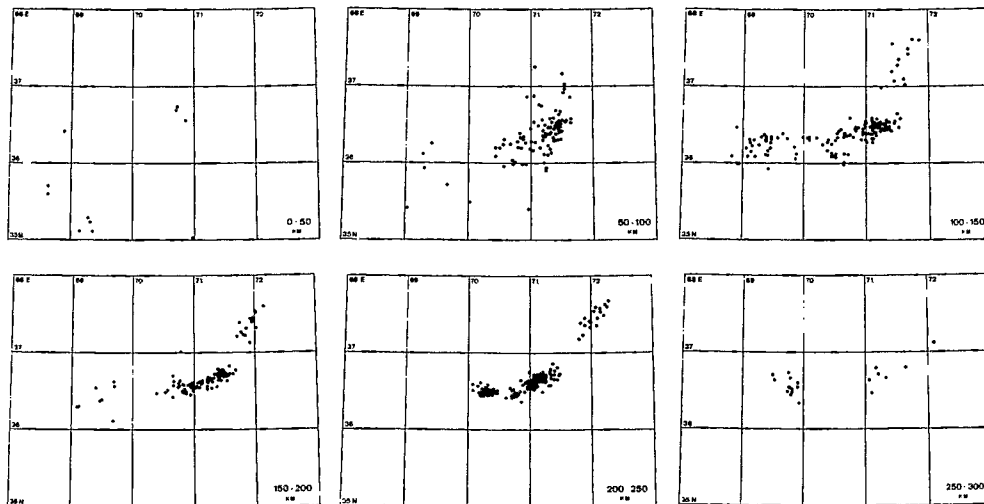


Fig. 5. Map views of the best locations of 1977. Events are divided into 50-km depth intervals.

## Results

### Mapping Techniques

The configuration of the zone, as revealed in each microseismic study, is displayed by plotting the recorded events in three orthogonal projections. The first consists of a series of plan views which divide the events into intervals of 50-km depth (Figures 5 and 7). The second is a series of vertical cross sections. Because of the basically accurate trend in the seismicity, we chose to divide the zone into several circular sections (Figure 4) and project the events onto planes bisecting the sections (Figures 6 and 8). Such projections are everywhere nearly perpendicular to the trend of the zone. In the third perspective the events are projected radially onto a vertical cylinder (H'H in Figure 4), resulting in a lateral section that is approximately parallel to the trend of the zone (H'H in Figures 6 and 8).

The events that met all the quality criteria established above are plotted as solid circles in these diagrams. While it is advantageous not to consider poor locations when describing the seismic trends of an area, it is important to insure that the criteria are not overly biasing the results. Therefore some events that did not meet all the criteria are included in the plots as open circles. First, shallow events with depths less than the distance to the nearest station but otherwise meeting the quality criteria are included in the plots for 1977. This is because this criterion would prohibit nearly all shallow seismicity regardless of how well recorded it is and would thus give a false impression of complete shallow aseismicity. Second, since all the tests described above were based on the 1977 array, the strict application of the criteria to the results of previous studies may be questionable. The configuration of the 1966-1967 [Roeker et al., 1980] array, for example, is somewhat different from that of 1977. Also, while the configuration of the 1976 array is

similar to that in 1977, the uncertainty in the arrival times is somewhat greater owing to the reading techniques used. Therefore in plotting the events from these other studies, the only restriction was that the Rms be less than 0.7.

### Description of the Zone

Because of our greater confidence in the 1977 results they provide the basis for our conclusions. Nevertheless, some of the conclusions from this study arise from defining regions of aseismicity. While considerable effort was spent verifying where events actually occur, the task of defining where they do not is more difficult. One can easily argue that 1 month of recording is not sufficient to sample the seismicity adequately. Fortunately, despite both the greater uncertainties and the fewer events in the other investigations of Hindu Kush seismicity, many of the gross aspects of the zone defined by the data from 1977 are apparent in the data from 1976, from 1966-1967, and from the teleseismic studies of Billington et al. [1977] and Santo [1969]. The agreement of all these results verifies the existence of features in the zone for at least 10 years.

In general, the intermediate depth seismicity of the Hindu Kush is confined to a small isolated area, roughly 700 km in extent and bounded on the west at about 69°E (Figure 1). The eastern boundary is beyond the limits of the local arrays, but teleseismic results show the intermediate seismicity ceases at about 75°E [Billington et al., 1977, Figures 2 and 3]. On the whole, the zone is grossly planar and steeply dipping, but several unusual features can be resolved with the 1977 data.

With the exception of some activity in the westernmost part of the zone, there is very little seismicity between 0- and 70-km depth (Figures 6 and 8, Roeker et al. [1980, Figures 2 and 3], Billington et al. [1977, Figures 2, 3, and 4], and Santo [1969, Figure 9]). Krestnikov and Wersesov [1964] inferred that the depth of the Moho is about 65-70 km for at least parts of this region. Therefore the

relatively aseismic region seems to correspond to the crust, with activity beginning abruptly in the mantle below.

The entire zone can be separated into two

regions of activity: one north of 37°N trending to the northeast and another south of 37°N aligned approximately east-west (Figure 5). At depths greater than about 100 km there is a

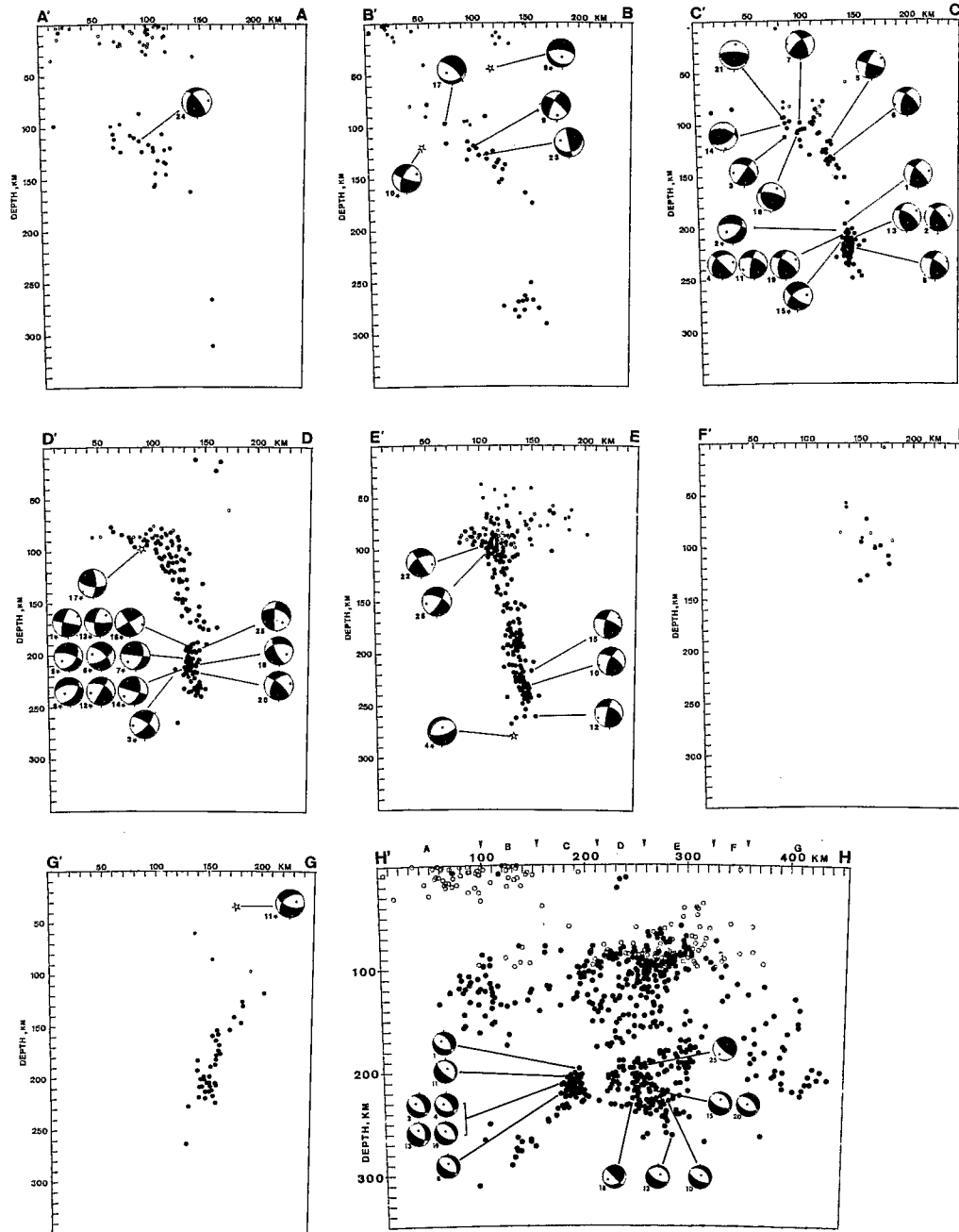


Fig. 6. Projections of 1977 hypocenters and fault plane solutions onto planes perpendicular to the zone (A'A - G'G) and onto a cylindrical surface parallel to the zone (H'H). In each of the sections perpendicular to the zone the northernmost side is marked by the unprimed letter. In the parallel section H'H, H marks the easternmost point, and the boundaries of the perpendicular sections are plotted above the figure. Solid circles represent locations which passed all of the quality criteria. Open circles represent events which passed all of the criteria with the exception of being recorded by a station whose epicentral distance was less than the depth of the event. Fault plane solutions are plotted in back sphere projections. Dark quadrants include compressional first motions, and white dilatational. T axes are plotted as open circles, and P axes as solid circles. Starred solutions are those determined with data from the WWSSN. All others were determined with local data.

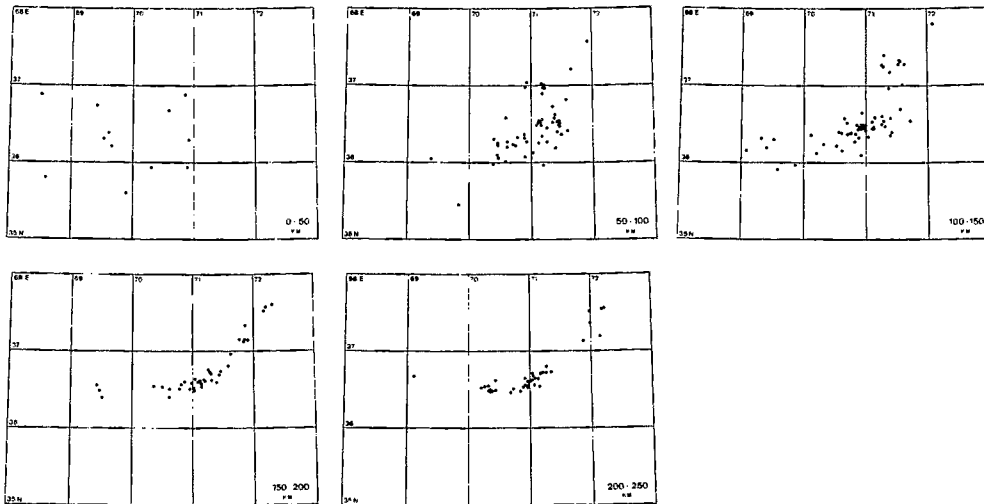


Fig. 7. Map of the best locations of 1976. Events are divided into 50-km depth intervals.

rather wide ( $\sim 50$  km) gap between these seismic regions, which appears in all of the local results (Figures 5, 7, and 9). The FF' cross section in Figures 6 and 8 and Figure 3 of Roecker et al. [1980] shows that this gap is well defined at depths greater than 150 km. The lateral projections show some curvature in this gap above 150 km and suggest that it extends down from as shallow as 100 km depth (Figure 9, H'H in Figures 6 and 8, and Roecker et al. [1980, Figure 3]). The seismicity shallower than 100 km that connects these two active regions north and south of  $37^\circ\text{N}$  seems to occur in a restricted area roughly 70 km long and 30 km in both width and depth.

The seismic zone south of  $37^\circ\text{N}$  can be further divided into two regions: a shallower one between 70- and 170-km depth and a deeper one between 180- and 300-km depth. Only one microearthquake was located deeper than 300 km for the entire zone. The gap between them is about 70 km wide in the west and narrows in the east to about 15-20 km near  $70.7^\circ\text{E}$  (Figure 9, H'H in Figure 6 and 8, and Roecker et al. [1980, Figure 3]). This gap is evident in Figures 3 and 4 in Billington et al. [1977], but unfortunately, the entire southern region was plotted on one projection, and identification of this gap in the west is impossible. Santo [1969, Figure 9] shows no real aseismic gap, but he notes a pronounced minimum of events at 160-km depth. We note that when viewed on lateral sections (HH' in Figure 6), the entire southern region seems to plunge west at roughly  $20^\circ$ . This observation is based on the apparent trends of the aseismic boundaries which define the shallower and deeper regions.

In cross section the shallower seismicity defines in the southwestern region a broad zone about 40 km in width (particularly CC', DD', and EE' in Figures 6 and 10). Even with the estimated errors for the locations this shallower region must be at least 30 km thick. In the far west the zone dips north at about  $45^\circ$  and becomes progressively steeper to the east. Although the seismicity appears to be continuous in the shallower region, there seems to be

a relative sparseness in activity roughly 30 km wide centered at about  $70.2^\circ\text{E}$ .

The deeper seismicity defines a consistently narrow zone (15-20 km wide) which has a nearly vertical dip (Figures 6 and 8, Roecker et al. [1980, Figure 3], and Billington et al. [1977, Figure 3]). Given the errors in locations, however, this zone could be somewhat thinner. In cross section the deeper events in the west seem to be more scattered than in the center of the zone, but as discussed above, the locations there are less precise.

In all of the local results a gap in the seismicity, which is about 15 km wide, appears at  $70.6^\circ\text{E}$  at about 200 km depth (Figs. 5, 7, and 9 and Roecker et al. [1980, Figure 2]). This gap also appears in Figure 6 of Billington et al., but the low density of events to the west of the gap makes its appearance less dramatic. The events east of 200- and 250-km depth near this gap between  $70.8^\circ\text{E}$  seem to concentrate (Fig. 5), but the possible gap between these and the events further east is too small to resolve with the present data. This concentration is especially important because it contains most of the events with fault plane solutions determined with the WWSSN.

Perhaps the most curious trend in the seismicity of the deeper region is the trail of events that extends downward and to the west of the concentration at  $70.3^\circ\text{E}$  (HH' in Figures 6 and 8). The narrowness of this trend when viewed from any angle suggests that the events are confined to a tube of activity which branches off from the concentration to the east.

Because the region to the north of  $37^\circ\text{N}$  is outside the 1977 array, any fine details of this seismic zone are more difficult to resolve. However, the gross trend of the zone shows a dip of about  $45^\circ$  to the southeast at 150-km depth that becomes almost vertical at 200-km depth (G'G in Figures 6 and 8, and Roecker et al. 1980, Figure 3]. Therefore this zone dips in nearly the opposite direction from that in the southern zone. This reversal in dip is also evident in Figure 5 of Billington et al., but they showed no reliably located events at



depths greater than about 170 km. By contrast, the 1977 results show microearthquakes to depths of about 240 km, with one event as deep as 260 km.

Although the Hindu Kush seismic zone is grossly planar and steeply dipping, in detail it is highly contorted and consists of several zones separated by gaps of aseismicity. Two of the most prominent gaps - one that separates the regions north and south of 37°N (Figures 5 and 9) and another that separates events deeper and shallower than about 160 km depth (Figure 9

and AA', BB' and HH' in Figure 6) - serve as boundaries between regions distinctly different in dip and breadth. A third gap, in the deeper region at 70.7°E (Figures 5, HH' and Figures 6 and 9) does not separate zones which show distinct qualities in spatial distribution of events but, as discussed below, seems to separate regions with different fault plane solutions. The consistency of the patterns obtained from studies made in the last few years, with both locally and teleseismically recorded data, confirms that these gaps have

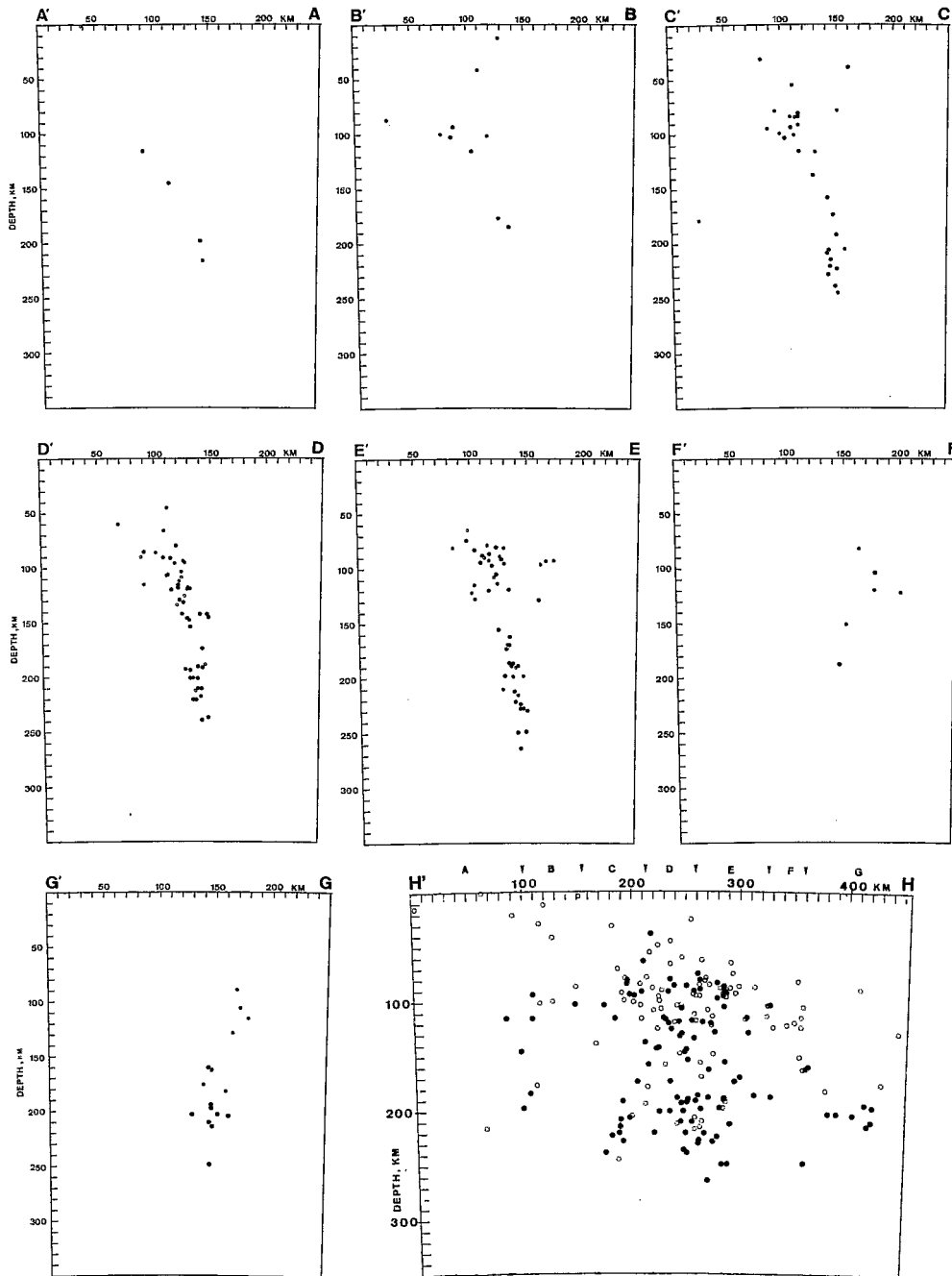


Fig. 8. Projections of the 1976 locations onto planes perpendicular and a cylinder parallel to the trend of the zone. The sections are the same as those used for the 1977 data (Figure 6). Hypocenters which passed all the quality criteria are plotted as solid circles. Open circles represent all of the events which have Rms residuals less than 0.7 but did not pass all the criteria.

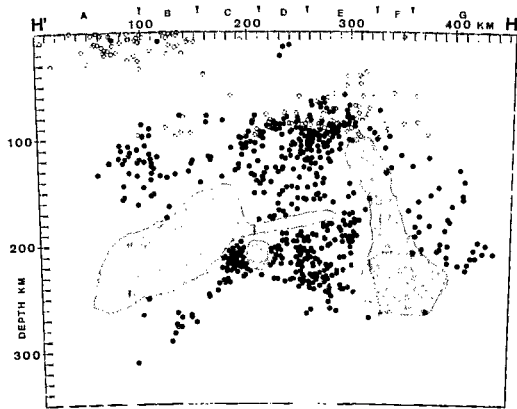


Fig. 9. Gaps in activity. HH' from Figure 6 is plotted without fault plane solutions but with gaps discussed in text shaded.

been real features in the Hindu Kush for at least the past 10 years. Moreover, their clear role as boundaries between regions of distinct qualities provides an argument for claiming that they may have existed for thousands of years and perhaps longer.

#### Fault Plane Solutions

Although the distribution of stations in 1977 proved adequate for determining locations over a wide area, the hypocentral regions for which well-constrained fault plane solutions could be determined were more restricted. Nevertheless, because of the large number of events recorded with data from the local stations, we were able to determine 26 relatively well constrained solutions for individual earthquakes in various places in the zone (Figure 10 and Table 2). The data were supplemented by first-motion readings from the Soviet station at Khorog [see Roecker et al., 1980]. Two composite solutions were made for events in regions where we could not obtain a solution for an individual earthquake (B and C in Figure 10 and Table 3). The purpose of these solutions is to show that the earthquakes of these regions have radiation patterns grossly consistent with those observed with WWSSN stations rather than implying the orientation of any axis or nodal plane. Composite fault plane solutions were, as a rule, avoided in this study. There are large variations among the well-constrained individual solutions for events in relatively small regions within the Hindu Kush, so that a composite solution will most likely misrepresent the patterns that exist. Fault plane solutions were also determined for 17 events using teleseismic recordings at WWSSN stations (Figure 10 and Table 4). While the addition of these solutions extends the regions represented by fault plane solutions, there are unfortunately few places where solutions based on local and teleseismic data overlap.

Giving a quantitative description of how well constrained a certain fault plane solution is or estimating the exact errors involved in the orientations of the nodal planes and axes requires several subjective decisions. Rather

than attach uncertainties to the parameters for each solution given in Tables 2 and 4, we present all the data used in determining the fault plane solutions in lower hemisphere plots (Figure 10).

As in previous investigations of fault plane solutions of the Hindu Kush [Billington et al., 1977; Isacks and Molnar, 1971; Ritsema, 1966; Shirokova, 1959; Soboleva, 1968a,b, 1972; Stevens, 1966], the solutions generally indicate thrust faulting with nearly vertical T axes. This type of solution is similar to that for intermediate depth earthquakes at island arcs [Isacks and Molnar, 1971]. There are, however, some significant variations that we explore by plotting the fault plane solutions in various orientations on the seismicity maps and profiles (Figures 6, 8, and 11-14).

Local solutions. Plotted in plan view (Figure 11), the solutions for events with depths less than 170 km show considerable scatter, much more scatter than is typical of island arcs. Although most display thrust faulting, solutions 23 and 24 have large strike slip components, and solutions 9, 21, and 14 indicate normal faulting. One might expect some scatter in these solutions because of the highly contorted nature of the shallow region. When plotted on the cross sections (Figure 6), many of the solutions seem to have either one nodal plane or the T axis parallel to the dip of the zone. One possible explanation for this duality is that events with nodal planes parallel to the zone occur along the boundary between two plates of lithosphere, while those with downdip T axes occur within a subducted slab of lithosphere. This observation is not consistent for all events, however, and the lack of sufficient data makes the explanation arguable. In any case the stress field in the shallow region appears to be too complex to be explained in a simple manner.

In contrast to the shallower region, solutions for events in the region below 170 km are much more consistent with one another. The solutions for the seven events (1, 2, 4, 8, 11, 13, and 19) in the concentration west of  $70.6^{\circ}\text{E}$  are essentially the same (Figure 12). The T axes lie within the plane of the zone and plunge to the west at an angle of about  $45^{\circ}$ . There appear to be some exceptions to this pattern, shown by the composite solution A (Figure 10), made using events in this region, for which there are some apparently inconsistent first motions.

Most of the solutions for events east of  $71^{\circ}\text{E}$  have similar solutions to those west of  $70.6^{\circ}\text{E}$ , but two of them (18 and 25) indicate more southward plunging T axes (Figure 12). The composite solution B (Figure 10), made from events in this area, generally shows compressional first motions in the center and is consistent with reverse faulting. There are unfortunately no solutions for the concentration of events near  $70.8^{\circ}\text{E}$  (Figure 12), which is where several events with solutions using the WWSSN are located. A composite solution (C in Figure 10) made from locally recorded events in this area shows compressional first motions in the center of the diagram, but the nodal planes are poorly constrained.

Viewed on the cross sections (Figure 6), the nodal planes for the deeper events, although regular, do not seem to align with any trend in seismicity, and so are not obviously related to any deep major faulting. A plot of the solutions on the lateral section (HH' in Figure 6) shows the P axes generally perpendicular to the seismic zone, and the T axes are consistently within it as at island arcs. The T axes, however, deviate from the downdip vertical direction by 20°-40°. The T axes for events in the cluster at 70.4°E seem to be parallel to the tube of seismicity that plunges to the west (HH' in Figure 6).

**WWSSN solutions.** As with the local solutions the T axes for most of the WWSSN solutions plunge steeply and lie within the zone. Similarly also, there is considerable variation in the solutions.

Most of the events for which WWSSN solutions are available are located in clusters (Figure 13). The radiation patterns for events within each cluster are generally similar to one another, but differ from cluster to cluster. In particular events near 36.4°N, 70.7°E and 210 km-depth (2, 5, 7, 8, and 14) all radiated compressional first motions to stations to the northwest and southeast, with some dilatations to the south and southwest (Figure 10). The solutions for events near 35.5°N, 70.9°E and 180-km depth indicate two trends. The events farther to the west (6 and 16) radiated compressions more to the south, and the quadrant with compressional first motion is aligned more east-west than for the solutions for events at 70.7°E. Events 1 and 13, at the eastern end of the cluster at 70.9°E, radiated dilatations to the southeast, and the zone of compressions tends to be aligned in a northeast-southwest direction. Events 3 and 12 radiated compressions to the east and west, and dilatations to the south. We note that these two events were located by the International Seismological Center in an area where we recorded no events. Solution 15, which is the only solution that overlaps with the local solutions at 70.4°E, generally has compressional first motions in the center of the diagram, but the nodal planes are poorly constrained. It is, in fact, possible to redraw this solution to look more like the local solutions (Figure 10). Event 4 radiated compressional first motions to the west, which are separated from dilatations to the east by a nodal plane that trends north-south. As mentioned above, this event is deep (~280 km) and is somewhat isolated from the rest of the events. Plotted in plan view (Figure 13), a pattern emerges where the P axes for the solutions rotate smoothly from a northeast-southwest orientation in the west to one that is more northwest-southeast in the east.

Viewed on the cross sections (Figure 6), two of the solutions (1 and 13) seem to have nodal planes aligned with the dip of the deeper zone. However, as in the local solutions, this observation is not applicable for most of the solutions. On the lateral section (Figure 14), there appears to be a systematic change in the plunge of the T axes from east to west. T axes for the five events (2, 5, 7, 8, and 14) at 70.7°E plunge about 70° to the north or north-

east. This cluster is just to the east of the gap at 70.6°E and contrasts with the westward plunging T axes of the local solutions west of the gap (H'H in Figure 6). East of 70.7°E, solutions 6 and 16 show nearly vertical T axes, and further east the T axes for events 1 and 13 plunge to the west, following the same pattern as the local solutions. The solution for event 12 also has a westward dipping T axis, while that for solution 3 is more vertical, but again there is no seismicity in this area to which these solutions can be related.

The four solutions for events shallower than 150 km (9, 10, 11, and 17) indicate large components of reverse faulting. These earthquakes are scattered throughout the zone, and events 9 and 11 apparently occurred in the crust. When plotted in plan view (Figure 11) or in cross section (Figure 6), the solutions for these events show no apparent consistency either among themselves or with the deeper events and seem to accentuate the variability of solutions for events shallower than 150 km, which were noted in the local solutions.

Fault plane solutions throughout the Hindu Kush are reminiscent of those for island arcs but show significantly more variation. When correlated with seismic trends, some patterns in the solutions emerge, but the stresses governing their orientations do not appear to be simple. Nodal planes of the solutions generally do not align with the dip of the zone, so there is apparently no major deep-seated faulting. The T axes for the deeper events lie in the plane of seismicity but do not plunge downdip. Instead, many plunge about 70° to the west, and align with the plunge of the tube of seismicity west of 70.5°E (HH' in Figure 6). As discussed below, there is some evidence that the aseismic gap at about 160-km depth indicates that the lower part of the slab has broken off from the upper part, at least in the west. The westward dipping T axes would then support the idea that the partially detached slab is hanging from the shallower region in a hingelike fashion. Resistance to subduction caused either by a pull from an eastern connection to the shallower zone or by some frictional drag due to flow of mantle material around an obliquely sinking lithosphere could cause the T axes to deviate from vertical. The exceptions to the westward plunging T axes that occur east of the gap at 70.6°E, where the T axes plunge to the east, is also evidence of a local perturbation in the stress field. This perturbation could indicate that the slab in this area is being torn apart by competing stresses. The origin of these stresses is uncertain, but the change in orientation of the axes about a relatively small gap suggests that the subducted lithosphere is discontinuous here.

#### Tectonic Interpretation

To discuss the Hindu Kush seismicity in the context of the India-Eurasia collision, we make some correlations between the trends of the zone and regional tectonics. In Figure 15 the projection of the seismic zone to the surface is drawn on a map depicting the major faults and some pertinent geology of the region.

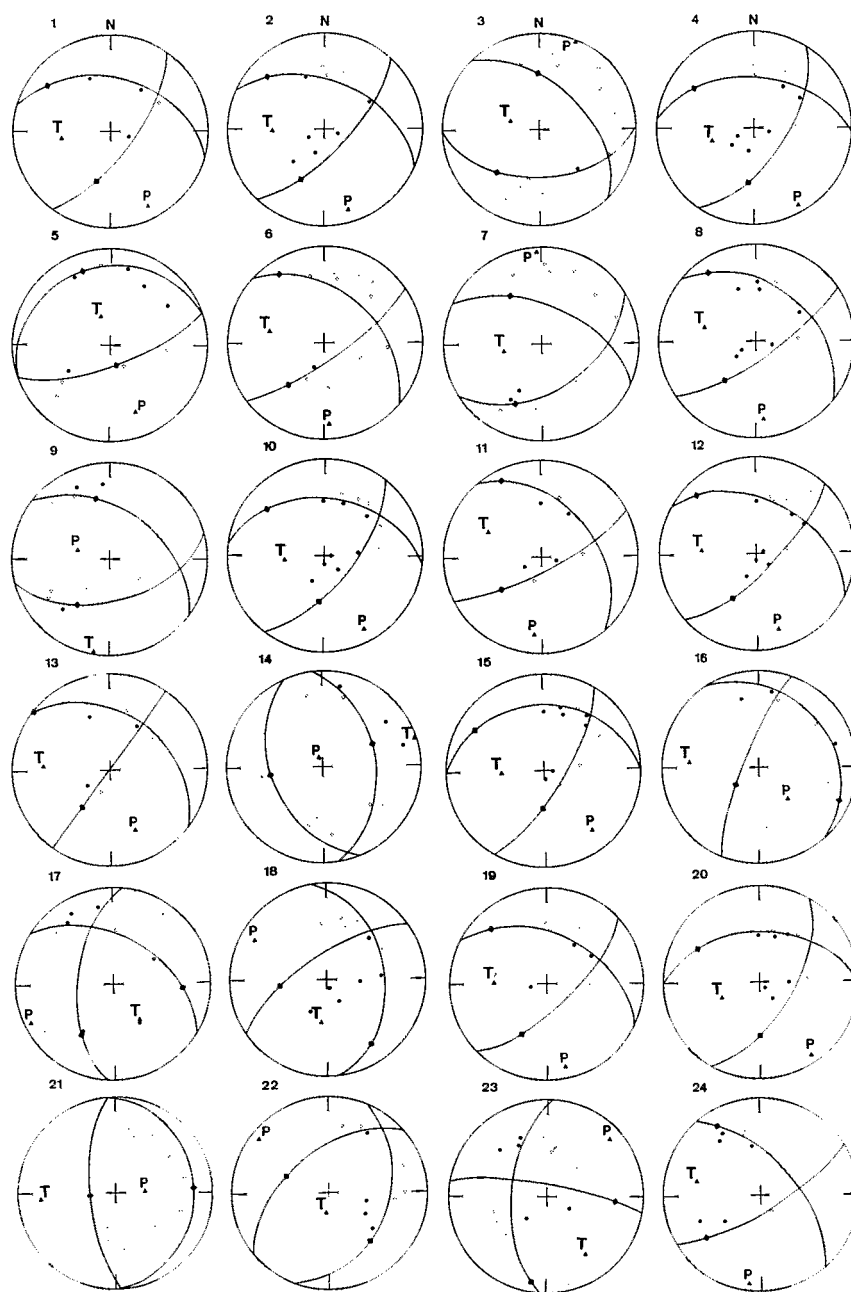


Fig. 10. Lower hemisphere fault plane solutions of all data used in this study. Solid circles represent compressional first motion, and open circles dilatations. Starred solutions are those using data from the WWSSN. Arrows on the WWSSN plots indicate S wave polarities, and crosses represent nodal readings. Solutions A, B, and C are composite solutions using local data.

### Tectonic Overview

As India approached Eurasia, subduction of the Tethys ocean beneath Eurasia apparently occurred along the Indus-Tsangpo suture zone [e.g., Dewey and Bird, 1970; Gansser, 1964, 1966]. The location of this suture east of  $76^{\circ}\text{E}$  is generally assumed to be quite simple with only a single belt of ophiolites [Gansser, 1966, 1977]. To the west, however, the location of the Indus suture is evidently not as simple. One candidate for the westward extension of the

Indus suture is the Dras volcanics that are found in the Ladakh region and can be traced westward almost continuously into Afghanistan [e.g., Gansser, 1977]. Mafic sequences in the Kohistan Himalaya south of the Dras volcanics, however, have been interpreted by Tahirkeili et al. [1977] as being suggestive of island arc crust. According to this interpretation, India would have been subducted at this island arc, and the Dras volcanics would mark the zone where a marginal basin between the arc and the rest of Asia was subducted (see also Burke et al. [1977]). In this region the Indus suture would be a broad

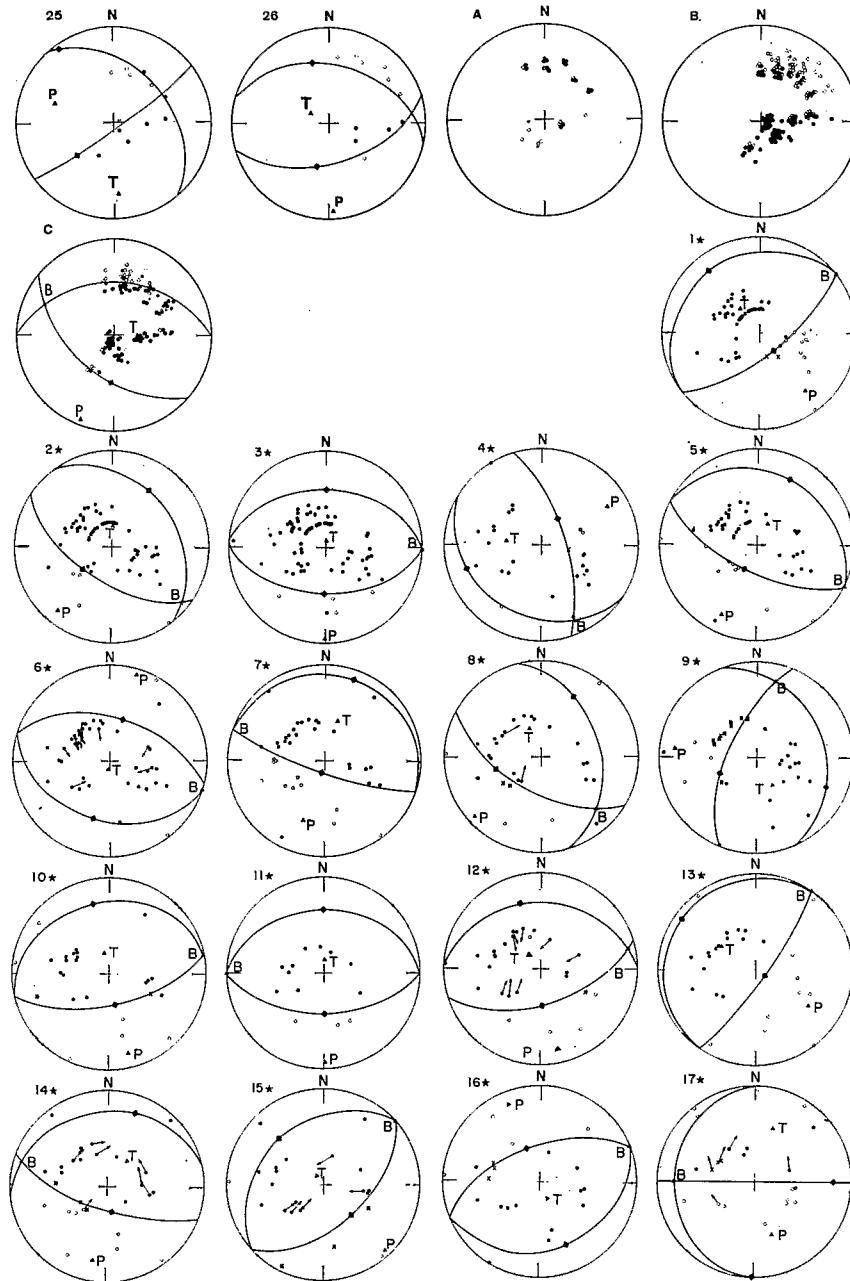


Fig. 10. (continued)

zone that includes both the arc terrain and the Dras volcanics.

The Dras volcanics seem to reach as far west as the Kunar fault, an active fault that is very clear on the Landsat imagery [Prevot et al., 1980]. The Kunar fault seems to terminate in the west near the Sarubi fault, an active right lateral strike slip fault [Prevot et al., 1980; Wellman, 1966]. Ophiolites have been found south and west of the Sarubi, and a mapping of them suggests that they were emplaced during the late Cretaceous or early Tertiary [Cassaigneau, 1979]. These ophiolites seem to be bordered on the west by the Chaman fault, an active left lateral fault than can be traced almost to the Gulf of Oman. West of the Chaman fault there have not seemed to be

ophiolites or other evidence of subduction since the mid-Cretaceous. At present, the Chaman fault appears to accommodate a substantial fraction of the slip between India and Eurasia [Auden, 1974; Chatelain et al., 1977; de Lapparent, 1972; Wellman, 1966]. Both the Chaman and Sarubi faults seem to terminate at the Panjer valley, through which, according to Wellman [1966], the east-west, right lateral Herat fault continues. The Panjer fault trends in a direction approximately parallel to the Kunar fault and is itself associated with ophiolite bodies [Gansser, 1977; Stöcklin, 1977].

In the north, crustal deformation, apparently due to the protrusion of India into Eurasia, essentially follows an arclike pattern

centered symmetrically at about 73°E. This region is laced with a series of southward dipping thrust faults. At least one of them, the Darvaz-Karakul fault, becomes a left lateral strike slip fault to the west [Kuchai and Trifonov, 1977]. To the east, most of the thrust faults abut against right lateral strike slip faults (e.g., the Karakorum fault) [Burtman et al., 1963; Peive et al., 1964; Ruzhentsev, 1963]. Some of these faults were active as early as in the Paleogene, while others appeared in more recent times [Peive et al., 1964]. The trend of the faults generally conforms to that of the Pamir mountain range. The Pamir, however, appears to be a westward continuation of the Kunlun, a late Paleozoic-early Mesozoic orogenic belt along the northern margin of Tibet (Morin [1979], and quoted by Molnar and Burke [1977]; Peive et al. [1964]). Subsequent right lateral faulting along the Karakorum and other faults seems to have displaced the Pamir 250 km north in relation to the Kunlun [Morin, 1979; Peive et al., 1964].

#### Inferences Derived From the Configuration of the Seismic Zone

The most general inference that one can make about the Hindu Kush seismic zone is that subduction has taken place. The narrow width and approximately planar character of the zone, along with its essential continuity to depths of 300 km, are indicative of anomalously low temperatures confined to a narrow, planar zone. Presumably, subduction of cold oceanic lithosphere into the warmer asthenosphere has occurred. For the rest of this discussion we take the general scenario of subduction as a starting point and elaborate on it as the additional complexities of the zone require. In particular, we are concerned with the rate and duration of subduction, the influence of the collision on the seismic zone, the possible

locations of sutures, and scenarios for emplacement.

#### Evidence For Times and Amounts of Subduction

With the exception of seismic activity beneath Burma, the Hindu Kush seismic zone is the only zone of intermediate depth activity near the boundary between India and Eurasia. This observation implies that the Hindu Kush was the scene of final subduction of oceanic lithosphere between India and Eurasia. If the subduction beneath the Hindu Kush was initiated prior to the collision, which occurred 45±10 m.y. ago [Gansser, 1966; Molnar and Tapponnier, 1975; Powell and Conaghan, 1973], the occurrence of earthquakes suggests that it has continued for some time after the collision as well.

Unlike most subduction zones, however, there are no active volcanoes and not even any known recent volcanic material above the seismic zone. Although a full understanding of calc-alkaline volcanism at island arcs is lacking, we note that such volcanism occurs at nearly every known actively subducting region. In western North America, volcanism and subduction seemed to have ceased at essentially the same time [Cross and Pilger, 1978; Snyder et al., 1976]. Although there are no active volcanoes in some portions of the Andes, beneath which subduction has taken place for a long time, most of the Andes experienced Pliocene or Quaternary volcanoes. Therefore we infer that since no volcanic rocks of late Cenozoic age have been reported anywhere along the Hindu Kush, subduction probably occurred only for a short duration.

One implication of a short duration is that if subduction was initiated a long time ago, for instance, 50 m.y. ago, cessation of subduction must also have occurred a long time ago. The existence of intermediate depth events would, however, seem to disallow that.

Table 2. Fault plane solutions determined with the local array data of 1977

NO	DATE	ORIGIN TIME	LATITUDE (°N)	LONGITUDE (°E)	DEPTH (KM)	F AXIS		T AXIS		N AXIS		POLE OF FIRST NODAL PLANE		POLE OF SECOND NODAL PLANE	
						AZ	PL	AZ	PL	AZ	PL	AZ	PL	AZ	PL
1	77/06/17	15:29	36°28'	70°14'	197	155	14	263	48	52	38	196	46	307	20
2	77/06/18	21:32	36°29'	70°19'	212	154	14	268	46	67	40	204	42	313	20
3	77/06/18	23:26	36°29'	70°38'	111	22	3	226	64	114	26	226	37	358	41
4	77/06/19	05:49	36°29'	70°23'	209	152	7	252	54	56	35	186	42	304	28
5	77/06/19	13:40	36°20'	70°04'	117	160	26	340	65	70	0	340	20	164	72
6	77/06/19	22:50	36°20'	70°39'	135	177	14	282	42	70	42	220	42	326	14
7	77/06/20	01:48	36°05'	70°26'	99	328	5	260	51	90	34	264	32	325	40
8	77/06/20	15:55	36°30'	70°23'	229	174	20	286	44	66	39	326	14	219	48
9	77/06/20	18:16	36°10'	69°24'	119	285	62	189	2	98	26	217	42	347	36
10	77/06/20	20:09	36°41'	71°05'	232	152	14	264	56	52	30	186	50	308	24
11	77/06/22	02:16	36°29'	70°20'	209	136	21	296	40	74	42	232	46	334	12
12	77/06/23	15:37	36°46'	71°11'	260	164	16	274	44	60	39	306	15	206	46
13	77/06/23	15:46	36°33'	70°17'	212	169	32	273	32	36	42	216	50	316	0
14	77/06/23	22:30	36°02'	70°43'	97	340	62	63	1	164	6	66	44	262	44
15	77/06/24	02:45	36°43'	71°07'	217	144	12	270	54	40	26	181	58	303	20
16	77/06/24	20:12	36°07'	70°43'	107	136	51	275	30	18	20	112	12	234	66
17	77/07/06	09:06	36°26'	69°29'	97	245	8	146	52	370	26	94	29	213	39
18	77/07/06	15:05	36°33'	70°57'	211	239	16	186	52	40	32	146	20	262	50
19	77/07/07	16:28	36°28'	70°20'	209	169	14	272	46	64	40	205	44	316	20
20	77/07/01	05:43	36°22'	71°00'	211	142	8	248	56	51	34	189	44	300	28
21	77/07/02	21:11	36°59'	70°43'	94	86	85	266	25	176	0	266	70	386	20
22	77/07/05	18:21	36°24'	71°30'	96	308	8	183	73	40	15	141	35	231	51
23	77/07/04	20:41	36°12'	69°56'	128	48	14	146	28	294	58	189	10	94	30
24	77/07/07	16:48	36°03'	69°08'	112	189	9	282	24	82	56	230	30	329	16
25	77/07/09	17:22	36°35'	71°02'	197	168	37	177	26	60	41	229	46	324	6
26	77/07/11	11:02	36°26'	71°20'	164	178	2	297	72	84	16	245	34	186	50

Table 3. Events used in determining composite fault plane solutions.

Sol.	Date	Origin time	Latitude (°N)	Longitude (°E)	Depth (km)
A	77/06/18	10:03	36°31'	70°24'	221
	77/06/20	00:25	36°31'	70°18'	210
	77/06/22	03:30	36°28'	70°20'	208
	77/06/26	11:03	36°27'	70°22'	216
B	77/06/17	17:14	36°33'	70°57'	197
	77/06/19	01:47	36°44'	71°29'	194
	77/06/20	20:00	36°42'	71°06'	233
	77/06/21	21:33	36°33'	71°22'	160
	77/06/23	23:32	36°42'	71°22'	167
	77/06/26	15:05	36°33'	70°57'	212
	77/07/02	04:09	36°41'	71°04'	242
	77/07/02	14:21	36°28'	70°59'	231
	77/07/03	01:55	36°43'	71°14'	254
	77/07/06	04:54	36°33'	71°01'	204
	77/07/08	01:30	36°38'	71°09'	212
	77/07/08	05:25	36°40'	71°10'	224
	77/07/08	09:50	36°42'	71°14'	235
	77/07/10	08:05	36°40'	71°09'	226
C	77/06/21	05:33	36°29'	70°46'	204
	77/06/23	03:22	36°27'	70°46'	214
	77/06/23	12:14	36°33'	70°41'	205
	77/06/23	20:40	36°38'	70°46'	190
	77/06/25	12:40	36°36'	70°45'	168
	77/07/01	01:39	36°25'	70°43'	219
	77/07/01	15:39	36°37'	70°59'	230
	77/07/02	03:30	36°34'	70°40'	174
	77/07/07	06:20	36°25'	70°38'	229
	77/07/08	03:22	36°27'	70°57'	163
	77/07/12	08:05	36°28'	70°48'	203

In active subduction zones, such as the Japanese arc, the limit in the depth of seismicity occurs in lithosphere that has resided in the mantle for about 15 m.y. or less. We suspect therefore that if subduction of lithosphere beneath the Hindu Kush has ceased, it probably could not have done so earlier than 20 m.y. ago. In fact, since the upper boundary of the seismicity seems to coincide with the depth of the Moho, it is possible that subduction has ceased very recently or is continuing aseismically through a relatively weak lower crust. The continuation of subduction would require that continental lithosphere is being subducted, a situation which might account for the broader zone of seismicity at depths shallower than 170 km.

Although it is difficult to place a precise limit on the duration or on the times of subduction, we can place lower bounds on values associated with these parameters. First the above observations taken together suggest that subduction beneath the Hindu Kush most likely completely postdates the collision about 45 m.y. ago and was probably much more

recent. Since the trend of the seismic zone is approximately perpendicular to the direction of convergence between India and Eurasia, it is unlikely that subduction occurred at a rate exceeding the rate of convergence between these two continents, about 43 mm/yr [Minster and Jordan, 1978]. From the depth of the seismic zone we know that at least 300 km of lithosphere have been subducted. Therefore while the lack of volcanics suggests a short duration of subduction, the depth of seismicity indicates it must be at least 7 m.y.

If all of the convergence did not take place in the region of subduction, the subduction rate could perhaps have been slower, which would in turn result in a longer duration. It is unlikely that the rate of subduction could be very much less, however, because, for lower rates, subduction to such depths probably could not occur. From a study of seismic zones where the rates of subduction and age of subducted oceanic lithosphere is known, Molnar et al. [1979] deduced that the length of the seismic zone is approximately proportional to the rate of subduction times the square of the thickness of subducted lithosphere. If the age of the subducted lithosphere is less than about 100 m.y., the thickness of the lithosphere is proportional to the square root of the age, so that, approximately, length = rate  $\times$  age<sup>1/2</sup> [Molnar et al., 1979]. For oceanic lithosphere older than about 120 m.y., however, the thickness of the lithosphere is essentially constant ( $\sqrt{125}$  km, Parsons and Sclater [1977]), so that the length of the seismic zone is proportional to the rate of subduction. Thus for a length of 300 km the rate of subduction of old lithosphere should be at least 20 mm/yr [Molnar et al., 1979]. For a maximum rate of 43 mm/yr the age of the lithosphere at the time it was subducted beneath the Hindu Kush should have been greater than about 70 m.y.

We conclude that relatively old, and therefore cold and thick, oceanic lithosphere was subducted beneath the Hindu Kush for a short duration in the late Tertiary.

#### Influence of the Collision

Locations of the earthquakes indicate that at least in the south the lithosphere is sharply bent, going from a horizontal to a vertical disposition in a very short distance. Assuming that the upper seismic zone defines an approximately circular transition region between these dispositions, the radius of curvature for this region is about 100 km. For most subduction zones the radius of curvature is about 200 km [Isacks and Barazangi, 1977]. From the discussion above we suggest that the subducted lithosphere was relatively thick. Therefore if the lithosphere is continuous, a large bending moment, significantly greater than is evident in island arcs, must be applied to it to bend it so sharply. The gap between the events shallower and deeper than about 170 km may in fact represent a discontinuity in the lithosphere, so that at shallower depths the lithosphere does not necessarily curve significantly with increasing depth. The vertically dipping lower region would then have

broken off recently and would be sinking somewhat independently of the shallower region. In addition, there is a considerable change in the dip of this shallower region from east to west. Since the length of the slab is much shorter than at island arcs, where the slab seems to be continuous, the gravitational body force associated with such a short slab is probably inadequate to bend the plate or to break it off. We suspect that the protrusion of the Indian subcontinent has provided a dynamic push that has bent the underthrust slab and straightened up the eastern end of the zone. This conjecture is supported by the fact that the top of the seismic zone near 70 km extends to shallower depths as the zone becomes more vertical, as one might expect if the entire slab were being rotated to a vertical direction without sinking. Moreover, the projection of the seismic zone to the surface (Figure 15) is parallel to trends of folds and faults such as those in the Panjer and Kunar valleys, which apparently were also deformed by the protrusion.

#### Emplacement Scenarios

An implication of a short duration of subduction is that it is unlikely that the lithosphere beneath the Hindu Kush was once part of the Tethys ocean that was attached to India and subducted beneath Eurasia, unless we have overestimated the date of the collision. Subduction that postdates the collision and occurs over a short duration suggests that independent pieces of oceanic lithosphere, such as intracontinental or interarc basins, have recently been subducted beneath the Hindu Kush north of the Tethys suture [Khalturin et al., 1977]. In examining this proposal we discuss the implications of a spectrum of possible emplacement scenarios.

The problem of trying to determine where and from which direction subduction took place is complicated by the fact that two parts of the zone dip in nearly opposite directions. Any explanation that assumes subduction in only one direction must account for the complete overturn of some part of the downgoing slab, presumably by the underthrusting lithosphere dragging it through the asthenosphere [e.g., Billington et al., 1977]. Such a phenomenon may have occurred north of New Guinea, where the intermediate depth zone dips south under the

island, not northward beneath the volcanoes [Johnson and Molnar, 1972].

The observation that Eurasia moves slowly with respect to frames of reference in which either the relative motion of the hot spots or the net rotation of the lithosphere is minimized [Minster et al., 1974] suggests that Eurasia has not overridden a slab attached to it. Since any slab originally dipping to the south probably would at most be forced to a vertical position, and since the southern zone dips northward, subduction from the north alone is unlikely.

In contrast, India moves rapidly with respect to such frames. As noted above, we infer that the protrusion of a northward moving Indian lithosphere is probably responsible for the partial straightening of the southern zone of subducted lithosphere. If one assumes that subduction occurred entirely from the south, this line of reasoning could be extrapolated to explain the overturning of the northeastern portion of the downgoing slab beneath the Pamirs [e.g., Billington et al., 1977]. Some evidence for this scenario is suggested by the trend of the seismic zone in this area, which conforms to the arc of deformation as defined by the southward dipping thrust faults in the Pamir. One consequence of such a scenario is that if the lithosphere were displaced northward sufficiently to overturn the slab, then the suture that formed when the last part of the basin was subducted, the Pamir suture, would be presently northwest of the seismic zone. The India-Eurasia suture zone is thought to be at or just south of the Kunar fault [Tahirkeli et al., 1977], which is nearly 300 km south of the seismic zone. The Kunar fault therefore could not have been the Pamir suture, and the oceanic lithosphere beneath the Pamir was not originally from the Tethys. Therefore regardless of whether or not subduction occurred entirely from the south, the existence of the intermediate depth events beneath the Pamir requires that an intracontinental (possibly interarc) basin originally lay north of the Kunar fault. Although we are aware of no evidence that disallows northward subduction beneath the Pamir and subsequent overturning of the zone, we think that the geologic evidence is more easily accommodated by a southward subduction beneath the Pamir.

Hence we think that a more likely scenario is

Table 4. Fault plane solutions determined with data from the WSSH.

No	DATE	LATITUDE (°N)	LONGITUDE (°E)	DEPTH (KM)	P AXIS		T AXIS		B AXIS		POLE OF FIRST NODAL PLANE		POLE OF SECOND NODAL PLANE	
					PL	AZ	PL	AZ	PL	AZ	PL	AZ	PL	AZ
1	64/01/28	36.48	70.95	197	26	140	64	320	0	50	22	320	72	140
2	65/03/14	36.42	70.65	205	15	219	72	2	8	127	30	32	58	241
3	66/06/06	36.43	71.12	221	5	180	85	0	0	90	40	0	50	180
4	67/01/25	36.71	71.60	281	24	60	60	276	17	155	64	32	22	252
5	69/03/05	36.41	70.73	208	20	205	70	25	0	115	45	25	65	205
6	69/08/08	36.44	70.86	196	7	16	83	196	0	106	52	16	38	196
7	71/08/06	36.42	70.73	207	35	198	55	18	0	108	10	18	80	138
8	72/01/20	36.39	70.72	214	10	228	64	339	22	134	30	28	50	256
9	72/06/24	36.28	69.69	47	17	276	62	152	20	14	22	112	56	246
10	72/11/16	35.67	69.91	120	18	166	72	346	0	76	27	346	63	166
11	73/10/12	37.68	71.88	35	10	180	80	0	0	90	35	0	55	180
12	73/10/17	36.38	71.11	211	15	168	75	322	10	76	30	342	60	176
13	74/05/13	36.54	70.96	197	35	124	55	304	0	34	10	304	80	124
14	74/07/30	36.42	70.76	209	24	190	63	35	10	285	20	19	67	168
15	74/12/10	36.48	70.47	213	10	137	80	317	0	47	35	317	55	137
16	75/03/03	36.45	70.92	187	15	337	75	157	0	67	30	157	60	337
17	75/05/14	36.08	70.90	97	42	161	42	18	20	270	0	0	70	90



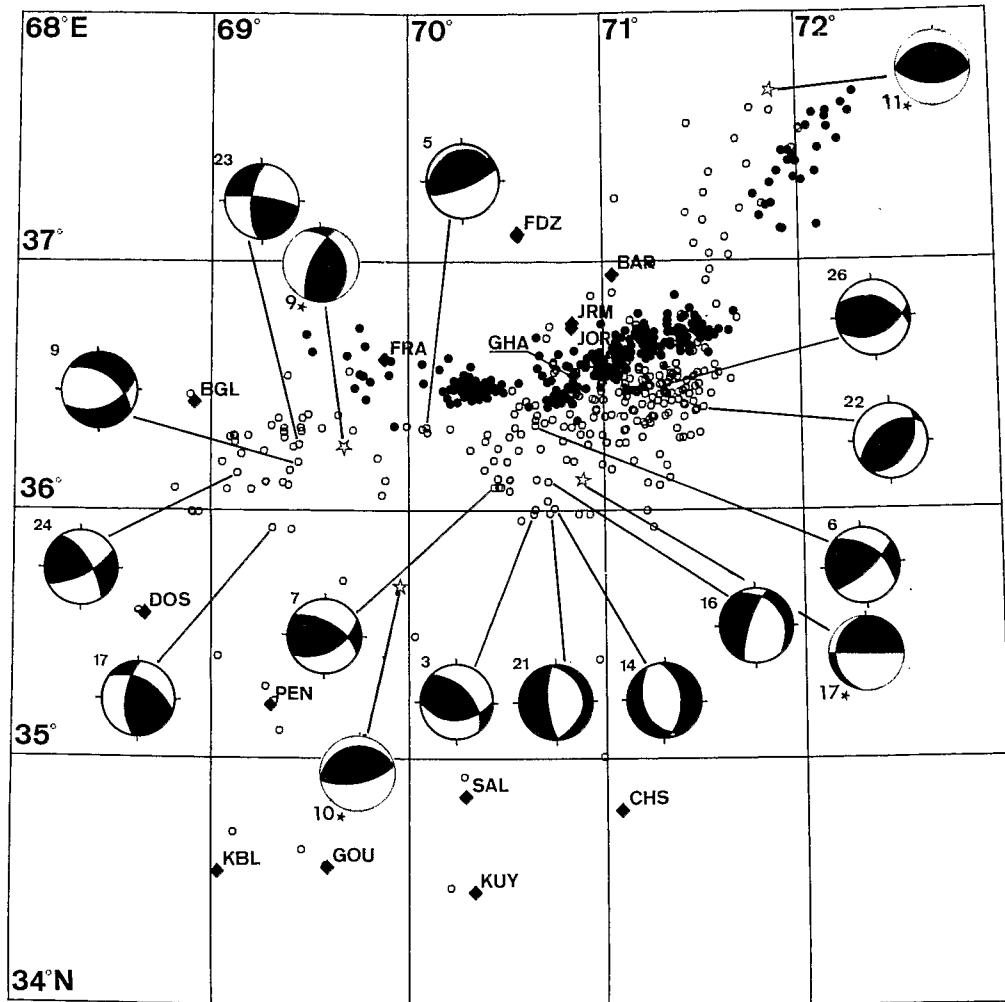


Fig. 11. Lower hemisphere projections in abbreviated balloon format of fault plane solutions for events shallower than 170-km depth using data from local and WWSSN stations. Locations of events using WWSSN data are plotted as stars. Dark quadrants represent compressional first motions, and white quadrants dilatations.

that two small ocean basins were subducted separately in opposite directions, one to the north beneath the Hindu Kush, and one to the south beneath the Pamir (see also Billington, et al. [1977], Malamud [1973] and Vinnik and Lukk [1974]). Evidence for subduction from the north beneath the Pamir consists of the following observations: first, the zone dips to the south. Second, almost all of the faults north of the zone indicate underthrusting to the south. By examining repeated facies of Cretaceous and Paleogene sediments, Peive et al. [1964] infer that at least 100 km of northward overthrusting has occurred along these faults. In the Garm region, just east of the Vakhsh overthrust, geodetic observations indicate active convergence of about 2 cm/yr [Konopoltsev, 1971] and an uplift of the south wall of a thrust fault at about 1 cm/yr [Finko and Enman, 1971; Nersesov et al., 1976]. A projection of the seismic zone to the surface lies near the Darvaz-Karakul fault, which changes from a southward dipping thrust in the north to a left lateral strike slip fault in the west [Kuchai and Trifonov, 1977]. Displace-

ment along the western part of Darvaz-Karakul seems to occur at about 1 cm/yr [Kuchai and Trifonov, 1977], and the accumulated displacement could be as much as 200 km [Zakharov, 1969]. Right lateral displacement of 250 km seems to have occurred along northeast trending faults east of the Pamir [Norin, 1979; Peive et al., 1964]. All of these data are consistent with a northward overthrusting of the Pamir onto the rest of the Eurasian landmass. Finally, thick marine sediments were deposited in the Tadjik depression north and west of the zone during the upper Cretaceous and Paleogene [Peive et al., 1964]. The Darvaz-Karakul fault seems to separate these sediments from Paleozoic deposits to the south and east. We note that subduction from the north requires a Pamir suture which lies far to the north of the India-Eurasia suture, and this in turn would imply that a marginal ocean basin, isolated within the Eurasian continent, once existed north of the Pamir.

The northward dip of the Hindu Kush seismic zone strongly implies that it formed by subduction from the south. Some geological

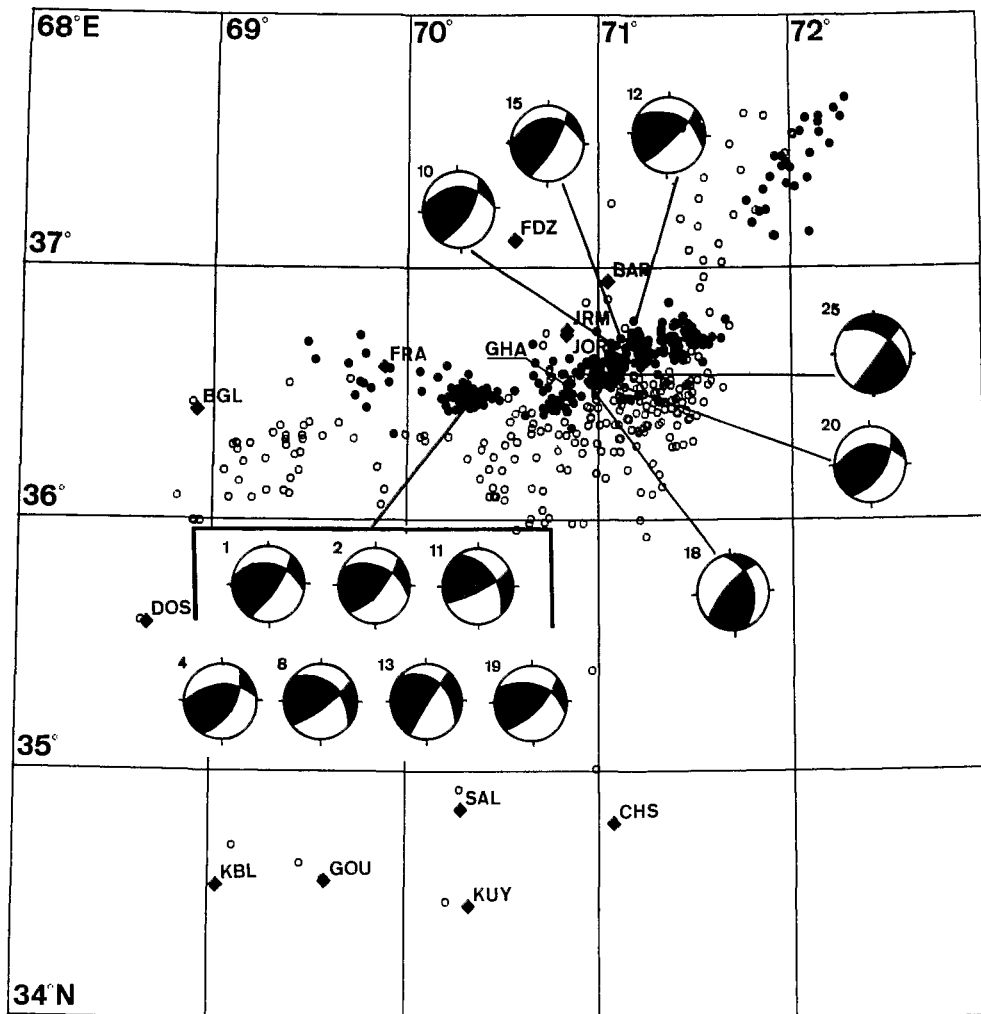


Fig. 12. Fault plane solutions using local data for events deeper than 170 km. Symbols as in Figure 11.

evidence exists that supports this direction of subduction, but the details of the emplacement are difficult to resolve. The surficial projection of the zone intersects the surface just south of the Panjer fault, making it a likely candidate for a suture zone. Ophiolites have been identified both on the Panjer and at least as far as 300 km to the south of the Panjer [Cassaigneau, 1979; Gansser, 1977; Stöcklin, 1977]. These latter ophiolites are bordered on the west by the Chaman fault, which apparently terminates at its intersection with the Herat fault in the Panjer valley. Such a geometry is suggestive of a system analogous to a trench-transform system. The Chaman fault has been active at least since some time in the Tertiary, and although the data are not conclusive, there may have been as much as 300-500 km of left lateral displacement along it [Auden, 1974; de Lapparent, 1973; Wellman, 1966]. A hypothetical extension of the fault past its termination aligns approximately with the western edge of the intermediate depth seismicity.

These observations, however, do not prove that subduction took place at the Panjer fault. The ophiolites south of the Panjer were apparently emplaced in the late Cretaceous or

early Tertiary [Cassaigneau, 1979; Gansser, 1977; Mattauer et al., 1978], which is too early to be associated with the final closure of a basin whose lithosphere now contains the Hindu Kush seismicity. Moreover, the ophiolites in the Panjer valley are of uncertain age and not well studied.

A second possibility for the suture zone is the Kunar fault and its extension east into the Hazara region north of the Kohistan Himalaya. From the geology of the region further north, Tahirkeili et al. [1977] suggested that an interarc basin was subducted at the Kunar fault after the collision with India. The projection of the seismic zone is approximately parallel to the trend of the Kunar fault but would imply that thrusting occurred on a plane dipping at about 20° between 0- and 70-km depth. Fault plane solutions of large events in the Himalaya are consistent with such a dip [e.g., Molnar et al., 1977], but a study of microearthquakes near the Kunar fault does not reveal a simple fault dipping northward [Prevot et al., 1980]. Again, this evidence is inadequate to prove that the lithosphere in which the Hindu Kush earthquakes occur was subducted here.

In any event, subduction beneath the Hindu Kush from the south seems likely, even if the suture zone cannot as yet be recognized with certainty.

Although the possibility of oppositely subducting lithosphere has been proposed before from other studies of seismicity, differences in the data resulted in different interpretations. In the teleseismic study of Billington et al. [1977], such a scenario was partially dismissed because the results implied that the two zones would somehow become contiguous after the collision. The microearthquake results, however, show a considerable gap between the regions. Therefore even though the simultaneous subduction of lithosphere in different directions within a relatively small area may seem unusual, the gap between them indicates that some spatial independence between the neighboring basins could have existed.

The earthquake locations also suggest that the sutures associated with subduction of the two basins lie on opposite sides of the Pamir-Hindu Kush orogenic belt. Since this belt formed in the late Paleozoic or early Mesozoic and therefore predates subduction, there must have been two oceanic basins separated by the Pamir-Hindu Kush belt regardless of the direction of subduction. On the basis of these

observations we suggest that the subduction of two oceanic basins in opposite directions beneath the Hindu Kush and Pamir is both plausible and likely.

Subduction of isolated basins probably has been quite common in the tectonic evolution of orogenic belts. As Arabia and Africa continue to converge with Eurasia, isolated basins such as those beneath the Black Sea and Caspian Sea probably will eventually be subducted. They could well be future analogues for the kind of subduction beneath the Hindu Kush and Pamir. For a brief time they will give rise to intermediate and possibly deep earthquakes in isolated areas far from the main suture zones, where thousands of kilometers of oceanic lithosphere were subducted. Clearly, the existence in the past of such basins and their subsequent subduction will cause complexity that will make the unraveling of geologic history of orogenic belts much more complicated than standard two-dimensional cartoons imply.

Summary

Owing to the high activity of the Hindu Kush seismic zone the microearthquake investigations of 1976 and 1977 recorded a substantial number of earthquakes. From a series of tests designed

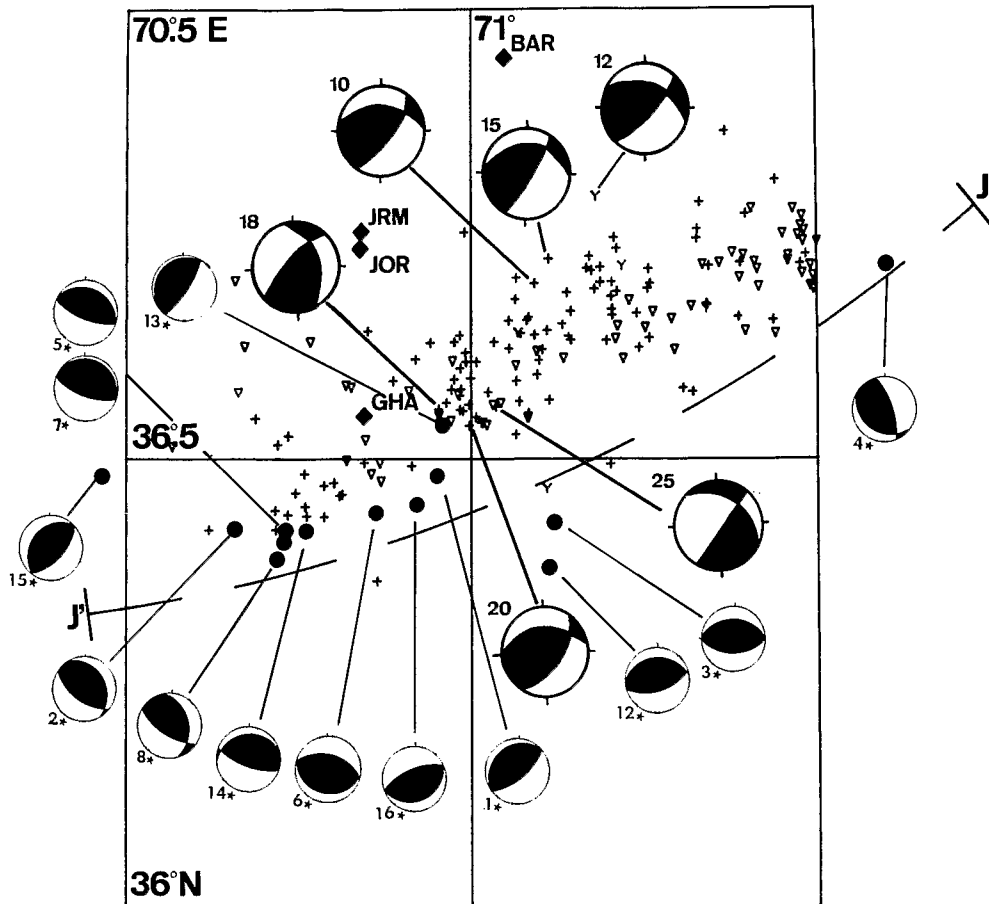


Fig. 13. Fault plane solutions using WWSSN data for events deeper than 170 km. Solutions for locally recorded events occurring in the area are plotted as well. The line J'J is a section of H'H used to plot the solutions in a lateral projection parallel to the zone. Symbols as in Figure 11.

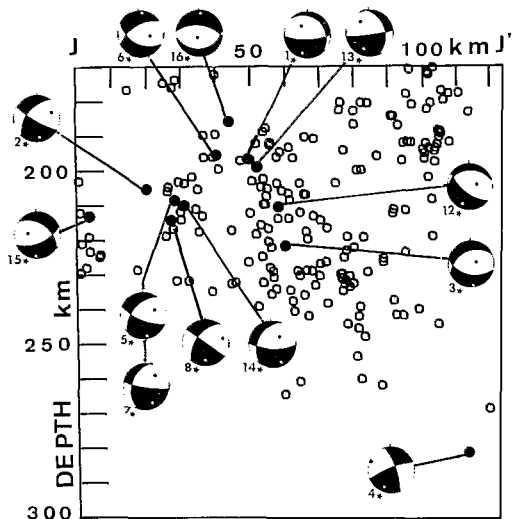


Fig. 14. Back hemisphere projections of fault plane solutions using WWSSN data onto a lateral section parallel to the zone. Location of the J'J section is given in Figure 13.

to evaluate different sources of uncertainty, quality criteria were developed for estimating the precision of the location of these events. From the 1200 events for which locations could be obtained, application of the criteria allowed us to cull out 600 well-located events, with uncertainties in epicenter of about 5 km and in depth of 10 km. These 600 events were used to define the seismic zone in some detail. While the definition of a seismic zone with data from a temporary network carries the stigma of inadequate sampling, many of the features revealed by the 1977 study are reflected in the microearthquake studies of 1976 and 1967-68 [Roecker et al., 1980] and in the teleseismic results of Billington et al. [1977] and Santo [1969]. In fact, the large number of earthquakes in the 1977 study accentuated many features such as a bend in the zone at shallower depths and aseismic gaps, which went largely unnoticed in previous studies.

We find that the crust from 0- to 70-km depth is essentially aseismic. Below the crust the seismic zone in the upper mantle is separated into three regions by two prominent aseismic gaps. A 70-km gap separates a southward dipping region beneath the Pamir from a northward dipping one beneath the Hindu Kush. A gap in seismicity beneath the Hindu Kush further separates seismic regions deeper and shallower than about 170 km from one another. The deeper region is characterized as a narrow (15-20 km) vertically dipping zone, while the shallower region is broad and dips at progressively steeper angles from west to east. The differences in dip and breadth of these regions makes the long-term role of the aseismic gaps as boundaries viable.

Fault plane solutions for the ocean events, determined with both local and WWSSN data, reveal T axes generally lying in the plane of seismicity and P axes generally perpendicular to the plane, which is similar to solutions in island arcs. In contrast to island arcs the T

axes are not always parallel to the dip of the zone, and there seems to be substantial variation in their orientation. Much of this variation occurs on opposite sides of a resolvable gap in activity of about 15-km width in the deeper region at about  $70.6^{\circ}\text{E}$ . To the west of this gap, T axes plunge to the west. On the other side of the gap, T axes plunge to the east and, further east, become progressively more westward plunging. In the western end of the deeper seismic zone, activity seems to be confined to a tube which dips to the west, and the T axes west of the  $70.7^{\circ}\text{E}$  gap are roughly parallel with this trend.

In contrast to the smooth variation of the solutions for deeper events, the fault plane solutions for shallower events show a great deal of scatter. A larger data set than is presently available may perhaps resolve a pattern in these solutions, but no consistent behavior is evident in the 1977 solutions.

On the basis of the essentially narrow and planar definition at the seismic zone to depths of 300 km, we infer that subduction of oceanic lithosphere has taken place beneath the Hindu Kush. Some bounds on parameters associated with this subduction can be made by considering the extent of the seismic zone and its relation to the tectonic environment. From the isolated nature of the seismic zone, from the occurrence of earthquakes at depths of 300 km, and from the absence of volcanic rocks above the zone it is likely that subduction occurred over a short duration and did not begin much before 20 m.y. ago. Subduction may actually be occurring today through a relatively weak lower crust. A recent history of subduction places an upper bound on the rate of subduction of about  $43$  mm/yr, while the depth of activity restricts this rate to be at least about 20 mm/yr. We infer that the oceanic lithosphere was probably greater than 70 m.y. old when subducted and therefore relatively thick. A comparison of the dips of the shallower and deeper zones suggests that the gaps between them near 170-km depth actually may represent a discontinuity in the lithosphere, and the change in dip of the shallower zone is most likely a result of the penetration of the Indian subcontinent into Eurasia.

By correlating the trend of the seismic zone with surficial geology we draw some inferences regarding the tectonic evolution of the region. Although the scenario given is not exclusive, we think that the available evidence is most easily accommodated by subduction of two separate basins in opposite directions. A projection of the seismic zone to the surface reveals some possible candidates for Hindu Kush - Pamir suture zones. North of the Pamir the seismic projection lies south of the Darvaz-Karakul thrust fault, which separates the thick Cenozoic marine deposits of the Tadjik depression in the west and north from Paleozoic deposits to the south and east. South of the Hindu Kush the projection lies just south of the Panjar fault, but the role of this fault as a suture is uncertain. Another candidate for Hindu Kush suture is the Kunar fault and its extension to the east, north of the Kohistan Himalaya, since it may have at one time been

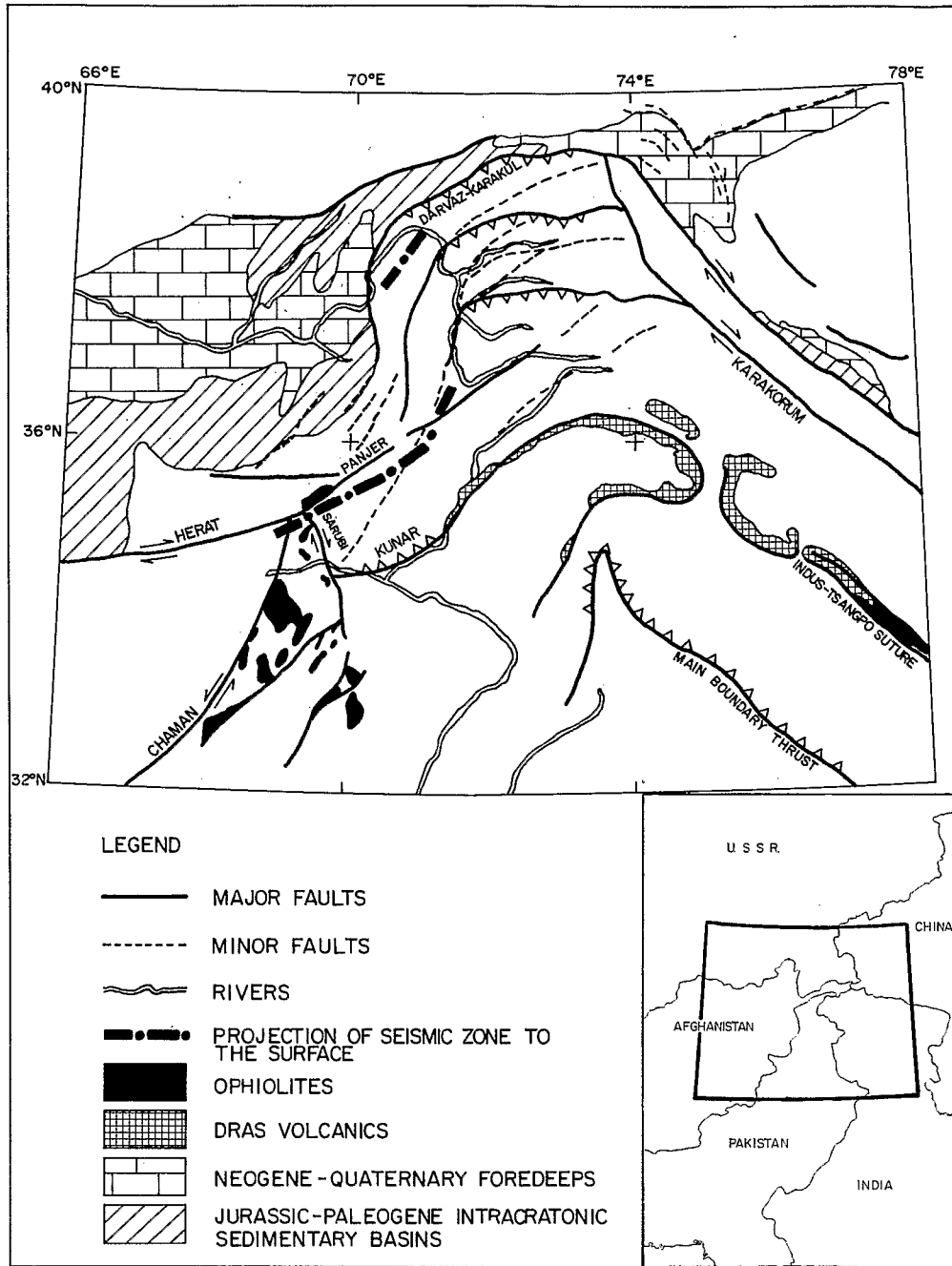


Figure 15. Map of major tectonic features of the Pamir-Hindu Kush region and their relation to a projection of the seismic zone to the surface. The projection of the zone was made by fitting a line to the trend of the shallower side of the zone above 170 km. Faults and geologic features are taken from maps compiled by Desio [1975], Gansser [1977], Peive et al. [1964], and Stöcklin [1977].

associated with subduction of a marginal basin [Burke et al., 1977; Tahirkeli et al., 1977].

While the unraveling of the history of the Pamir-Hindu Kush is rather complicated, we suggest that the geology and seismicity in this area may actually be a prototype of a type of complexity that will exist after basins such as those beneath the Black and Caspian seas are subducted and that has probably been common in collision zones.

**Acknowledgements.** We thank J. P. Carbonnel for assistance in both logistics and technical matters. We were ably assisted in the field by J. Frechet, M. Frogneux, X. Goula, M. Grosenbaugh, L. Jones, J. King, J. Maurer, R. Prevot, G. Suarez, and B. Tucker and Afghan engineers Kandari, Osman, Rabi, and Sharif. We appreciated the assistance and hospitality of J. Summers of the Afghan American Educational Commission and R. E. Gibson, H. Hafiz, A. S.

Saleem, and others of Kabul University. We thank Woodward Clyde Consultants and, in particular, W. Savage and D. Tocher for loaning us two Sprengnether instruments for the work in 1977. We thank D. Gubbins for assisting us in preparing the test made with a laterally heterogeneous structure. We also benefitted from discussion and encouragement from K. H. Jacob, V. I. Khalturin, A. A. Lukk, M. Mattauer, I. L. Nersesov, G. Perrier, F. Proust, T. G. Rautian, L. Seeber, O. V. Soboleva, and P. Tapponnier. We thank Kabul University for copies of seismograms from the station in Kabul, the Applied Seismology Group of the Lincoln Laboratory and Lamont-Doherty Geological Observatory for the use of the WSSN data and facilities, Lamont also for the use of data from the Tarbella Array, and the Institute of Physics of the Earth of the Academy of Sciences of the USSR for allowing us to examine records from Soviet stations in Tadjikistan. Finally we thank two anonymous referees for constructive criticism. This research was supported primarily by contract ATP No. 35-06 of INAG (Grenoble) and NSF grants EAR76-13367A01 and EAR78-13673 (MIT). The MIT group's part, however, was made possible by an H. O. Wood award from the Carnegie Institution in Washington and by an Alfred P. Sloan Fellowship.

#### References

- Armbruster, J., L. Seeber, and K. H. Jacob, The northwestern termination of the Himalayan mountain front: Active tectonics from micro-earthquakes, J. Geophys. Res., **83**, 269-282, 1978.
- Auden, J. B., Afghanistan-West Pakistan, Mesozoic-Cenozoic Orogenic Belts: Data for Orogenic Studies; Alpine-Himalayan Orogens, Geol. Soc. London Spec. Publ., **4**, 365-378, 1974.
- Billington, S., B. L. Isacks, and M. Barazangi, Spatial distribution and focal mechanisms of mantle earthquakes in the Hindu-Kush-Pamir region: A contorted Benioff zone, Geology, **5**, 699-704, 1977.
- Buland, R., The mechanics of locating earthquakes, Bull. Seismol. Soc. Amer., **66**, 173-188, 1976.
- Burke, K., J. F. Dewey, and W. S. F. Kidd, World distribution of sutures: The sites of former oceans, Tectonophysics, **40**, 69-99, 1977.
- Burtman, V. S., A. V. Peive, and S. V. Ruzhentsev, Main lateral faults of Tien Shan and Pamir, in Faults and Horizontal Movements of the Earth's Crust (in Russian), Academy of Sciences of the USSR, Institute of Geology, pp. 152-172, 1963.
- Cassaigneau, C., Contribution a l'étude des suture Inde-Eurasie; la zone de suture de Khost dans le Sud-Est de l'Afghanistan l'abduction Paleogene et la tectonic tertiaire, these de Docteur de 3<sup>eme</sup> cycle, Univ. des Sci. et Tech. du Languedoc, Montpellier, France, 1979.
- Chatelain, J. L., S. Roecker, D. Hatzfeld, P. Molnar, and G. Perrier, Etude seismologique en Afghanistan, Primiers resultats, C. R. Somm. Soc. Geol. Fr., **5**, 260-262, 1977.
- Cross, T. A., and R. H. Pilger, Constrains on absolute plate motions and plate interaction inferred from Cenozoic igneous activity in the western United States, Amer. J. Sci., 1978.
- de Lapparent, A. F., Esquisse géologique de l'Afghanistan, Rev. Geogr. Phys. Geol. Dyn., **14**, (2), 327-344, 1972.
- Desio, H. (ed.), Italian Expeditions to the Karakorum (K2) and Hindu Kush, vol. 3, Geology of Central Badakhstan (Northeast Afghanistan) and Surrounding Countries, 628 pp., E. J. Brill, Leiden, Netherlands, 1975.
- Dewey, J. F., and J. M. Bird, Mountain belts and the new global tectonics, J. Geophys. Res., **75**, (14), 2625-2647, 1970.
- Finko, Ye. A., and V. B. Enman, Present surface movements in the Surkhob fault zone (in Russian), Geotectonika, **5**, 117-125, 1971.
- Gansser, A., Geology of the Himalayas, 289 pp., Interscience, New York, 1964.
- Gansser, A., The Indian Ocean and the Himalayas A geological interpretation, Eclogae Geol. Helv., **59**, 831-848, 1966.
- Gansser, A., The great suture zone between Himalaya and Tibet - A preliminary account, in Himalaya: Sciences de la Terre, pp. 209-212, Centre National de la Recherche Scientifique, Paris, 1977.
- Isacks, B. L., and M. Barazangi, Geometry of Benioff zones: Lateral segmentation and downwards bending of the subducted lithosphere Island Arcs, Deep-Sea Trenches, and Back-Arc Basins, Maurice Ewing Ser., Vol. 1, edited by M. Talwani and W. C. Pitman, III, pp. 99-114, AGU, Washington, DC, 1977.
- Isacks, B. L., and P. Molnar, Distribution of stresses in the descending lithosphere from a global survey of focal mechanism solutions of mantle earthquakes, Rev. Geophys. Space Phys., **9**, 103-174, 1971.
- James, D. E., I. S. Sacks, E. Lazo L., and P. Araricio G., On locating local earthquakes using small networks, Bull. Seismol. Soc. Amer., **59**, 1201-1212, 1969.
- Johnson, T., and P. Molnar, Focal mechanisms and plate tectonics of the southwest Pacific, J. Geophys. Res., **77**, 1433-1438, 1972.
- Khalturin, V. V., T. G. Rautian, and P. Molnar, The spectral content of Pamir-Hindu Kush intermediate depth earthquakes, evidence for a high Q zone in the upper mantle, J. Geophys. Res., **82**, 2931-2943, 1977.
- Konopaltsev, I. M., Crustal movements in the Garm area, from the 1948-1970 measurements (in Russian), Geotectonika, **5**, 111-116, 1971.
- Krestnikov, V. V., and I. L. Nersesov, Relations of the deep structure of the Pamirs and Tien Shan to their tectonics, Tectonophysics, **1**, 183-191, 1964.
- Kuchai, V. K., and V. G. Trifonov, Young sinistral shearing along the Darvaz-Karakul fault zone, (in Russian), Geotectonika, **3**, 91-105, 1977.
- Lee, W. H. K., and J. C. Lahr, HYP071 (revised): A computer program for determining hypocenter, magnitude, and first motion pattern of local earthquakes, Open File Rep., **75-311**, U. S. Geol. Surv., Reston, VA, 1975.
- Lukk, A. A., and I. L. Nersesov, The deep Pamir-Hindu Kush earthquakes, in Earthquakes in the USSR in 1966 (in Russian), pp. 118-136, Nauka, Moscow, 1970.
- Malamud, A. S., Several regularities of the spatial distribution of the Pamir-Hindu Kush

- deep focus earthquakes (in Russian), Izv. Akad. Nauk Tadzh. SSR Otd. Fiz. Matematischeskikh Geol. Khim. Nauk, 4, 70-73, 1973.
- Mattauer, M., F. Proust, P. Tapponnier, and C. Cassaigneau, Ophiolites, obductions et tectonique global dans l'Est de l'Afghanistan, C. R. Acad. Sci., 287, 983-985, 1978.
- Minster, J. B., and T. H. Jordan, Present day plate motions, J. Geophys. Res., 83, 5331-5354, 1978.
- Minster, J. B., T. H. Jordan, P. Molnar, and E. Haines, Numerical modeling of instantaneous plate tectonics, Geophys. J. Roy. Astron. Soc., 36, 547-576, 1974.
- Molnar, P., and K. Burke, Penrose conference report: Erik Norin Penrose Conference on Tibet, Geology, 5, 461-463, 1977.
- Molnar, P., W. P. Chen, T. J. Fitch, P. Tapponnier, W. E. K. Warsi, and F. T. Wu, Structure and tectonics of the Himalaya: A brief summary of relevant geophysical observations, Colloques Internationaux du C.N.R.S., No. 268, Ecologie et Geologie de l'Himalaya, 269-293, 1977.
- Molnar, P., and P. Tapponnier, Cenozoic tectonics of Asia: Effects of a continental collision, Science, 189, 419-426, 1975.
- Molnar, P., D. Freedman, and J. S. F. Shih, Lengths of intermediate and deep seismic zones and temperatures in downgoing slabs of lithosphere, Geophys. J. Roy. Astron. Soc., 56, 41-54, 1979.
- Nersesov, I. L., T. V. Latynina, T. V. Guseva, N. Zharinev, and A. A. Khobotko, On the deformation of the earth's crust in the Surkhob fault zone (in Russian), Izv. Acad. Sci. USSR, Phys. Solid Earth, 12, 26-37, 1976.
- Norin, E., The relation between the Tibetan platform and the Tarim Basin, Submitted to Geol. Soc. Amer. Bull., 1979.
- Nowroozi, A. A., Seismo-tectonics of the Persian plateau, eastern Turkey, Caucasus, and Hindu Kush regions, Bull. Seismol. Soc. Amer., 61, 317-321, 1971.
- Nowroozi, A. A., Focal mechanism of earthquakes in Persia, Turkey, West Pakistan, and Afghanistan and plate tectonics of the Middle East, Bull. Seismol. Soc. Amer., 62, 823-850, 1972.
- Parsons, B., and J. Sclater, An analysis of ocean floor bathymetry and heat flow with age, J. Geophys. Res., 82, 803-827, 1977.
- Peive, A. V., V. S. Burtman, S. V. Ruzhentsev, and A. I. Suvorov, Tectonics of the Pamir-Himalayan sector of Asia, in Report of the Twenty Second Session, India, International Geological Congress, part XI, Himalayan and Alpine Orogeny, pp. 441-464, International Geological Congress, New Delhi, 1964.
- Powell, C. McA., and P. J. Conaghan, Plate tectonics and the Himalayas, Earth Planet. Sci. Lett., 20, 1-12, 1973.
- Prevot, R., D. Hatzfeld, S. W. Roecker, and P. Molnar, Shallow earthquakes and active tectonics in eastern Afghanistan, J. Geophys. Res., 85, this issue, 1980.
- Ritsema, A. R., The fault plane solutions of earthquakes of the Hindu Kush Centre, Tectonophysics, 3, 147-163, 1966.
- Roecker, S. W., O. V. Soboleva, D. Hatzfeld, J. L. Chatelain, and P. Molnar, Seismicity and fault plane solutions of intermediate depth earthquakes in the Pamir-Hindu Kush region, J. Geophys. Res., 85, this issue, 1980.
- Ruzhentsev, S. V., Transcurrent faults in the southeastern Pamir, in Faults and Horizontal Movements of the Earth's Crust (in Russian), pp. 115-127, Academy of Sciences of the USSR, Institute of Geology, Moscow, 1963.
- Santo, T., Regional study on the characteristic seismicity of the world, I, Hindu Kush region, Bull. Earthquake Res. Inst., Tokyo Univ., 47, 1035-1049, 1969.
- Shirokova, E. I., Determination of the stresses effective in the foci of the Hindu Kush earthquakes (in Russian), Izv. Akad. Nauk SSSR, Ser. Geofiz., 12, 1739-1745, 1959.
- Snyder, W. S., W. R. Dickinson, and M. L. Silberman, Tectonic implications of space-time patterns of Cenozoic magmatism in the western United States, Earth Planet. Sci. Lett., 32, 91-106, 1976.
- Soboleva, O. V., Special features of the directions of the principal stress axes in the foci of Hindu Kush earthquakes (in Russian), Izv. Acad. Sci. USSR, Phys. Solid Earth, 1, 71-78, 1968a.
- Soboleva, O. V., Effect of the asymmetry of the focal radiation upon the distribution of the displacements around the epicenter of a deep earthquake (in Russian), Izv. Acad. Sci. USSR, Phys. Solid Earth, 10, 45-56, 1968b.
- Soboleva, O. V., Method for unambiguous determination of the fault plane in the source using the Hindu-Kush zone as an example, (in Russian), Izv. Acad. Sci. USSR, Phys. Solid Earth, 1, 50-59, 1972.
- Stevens, A. E., S-wave focal mechanism studies of the Hindu Kush Earthquake of 6 July 1962, Can. J. Earth Sci., 3, 367-384, 1966.
- Stöcklin, J., Structural correlation of the Alpine ranges between Iran and Central Asia, in Livre a la Memoire de Albert F. de Lapparent, pp. 333-353, Société Géologique de France, Paris, 1977.
- Tahirkeili, R. A. K., M. Mattauer, F. Proust, and P. Tapponnier, Données nouvelles sur la suture Inde-Eurasie au Pakistan, in Himalaya; Sciences de la Terre, pp. 209-212, Centre National de la Recherche Scientifique, Paris, 1977.
- Vinnik, L. P., and A. A. Lukk, Velocity inhomogeneities of the upper mantle of Central Asia (in Russian), Dok. Akad. Sci. USSR, 213, 580-583, 1973.
- Vinnik, L. P., and A. A. Lukk, Lateral inhomogeneities in the upper mantle under the Pamir-Hindu Kush (in Russian), Izv. Acad. Sci. USSR, Phys. Solid Earth, 1, 9-22, 1974.
- Vinnik, L. P., A. A. Lukk, and I. L. Nersesov, Nature of the intermediate seismic zone in the mantle of Pamir-Hindu Kush, Tectonophysics, 38, T9-T14, 1977.
- Wellman, H. N., Active wrench faults of Iran, Afghanistan, and Pakistan, Geol. Rundschau, 55, 716-735, 1966.
- Zakharov, S. A., On the characteristic features of the geotectonics of the Tadjik depression, in Neotectonics and Seismotectonics of Tadjikistan (in Russian), pp. 3-19, Donish, USSR, 1969.

(Received April 23, 1979;  
revised November 1, 1979;  
accepted November 7, 1979.)